

Solitons and Nonlinear Dynamics in Dual-Core Optical Fibers

Boris A. Malomed

Department of Physical Electronics,

School of Electrical Engineering, Faculty of Engineering,

Tel Aviv University, Tel Aviv 69978, Israel

Laboratory of Nonlinear-Optical Informatics,

ITMO University, St. Petersburg 197101, Russia

Abstract

The article provides a survey of (chiefly, theoretical) results obtained for self-trapped modes (solitons) in various models of one-dimensional optical waveguides based on a pair of parallel guiding cores, which combine the linear inter-core coupling with the intrinsic cubic (Kerr) nonlinearity, anomalous group-velocity dispersion, and, possibly, intrinsic loss and gain in each core. The survey is focused on three main topics: spontaneous breaking of the inter-core symmetry and the formation of asymmetric temporal solitons in dual-core fibers; stabilization of dissipative temporal solitons (essentially, in the model of a fiber laser) by a lossy core parallel-coupled to the main one, which carries the linear gain; and stability conditions for \mathcal{PT} (parity-time)-symmetric solitons in the dual-core nonlinear dispersive coupler with mutually balanced linear gain and loss applied to the two cores.

The list of acronyms

1D: one-dimensional

2D: two-dimensional

BG: Bragg grating

CGLE: complex Ginzburg-Landau equation

CQ: cubic-quintic (nonlinearity)

CW: continuous-wave (solution)

GPE: Gross-Pitaevskii equation

GS: gap soliton

GVD: group-velocity dispersion

MI: modulational instability

NLSE: nonlinear Schrödinger equation

\mathcal{PT} : parity-time (symmetry)

SBB: symmetry-breaking bifurcation

SP: solitary pulse

SPM: self-phase modulation

VA: variational approximation

WDM: wavelength-division multiplexing

XPM: cross-phase modulation

I. INTRODUCTION

One of basic types of optical waveguides is represented by dual-core couplers, in which parallel guiding cores exchange the propagating electromagnetic fields via evanescent fields tunneling across the dielectric barrier separating the cores [1]. In most cases, the couplers are realized as twin-core optical fibers [2, 3], or, in a more sophisticated form, as twin-core structures embedded in photonic-crystal fibers [4]. Such double fibers can be drawn by means of an appropriately shaped preform from melt, or fabricated by pressing together two single-mode fibers, with the claddings removed in the contact area. Alternatively, a microstructured fiber with a dual guiding core can be fabricated and used too [5].

If the intrinsic nonlinearity in the cores is strong enough, the power exchange between them is affected by the intensity of the guided signals [6]. This effect may be used as a basis

for the design of diverse all-optical switching devices [7]-[13] and other applications, such as nonlinear amplifiers [14, 15], stabilization of wavelength-division-multiplexed (WDM) transmission schemes [16], logic gates [17], and bistable transmission [19]. Nonlinear couplers also offer a setup for efficient compression of solitons by passing them into a fiber with a smaller value of the group-velocity dispersion (GVD) coefficient: as demonstrated in work [18], the highest quality of the soliton's compression is achieved when two fibers with different dispersion coefficients are not directly spliced one into the other, but are connected so as to form a coupler (a necessarily asymmetric one, in this case).

In addition to the simplest dual-core system, realizations of nonlinear couplers have been proposed in many other settings, including the use of the bimodal structure (orthogonal polarizations) of guided light [20], semiconductor waveguides [21], plasmonic media [22–24], and twin-core Bragg gratings [25–27], to mention just a few. In addition to the ubiquitous Kerr (local cubic) nonlinearity of the core material, the analysis has been developed for systems with nonlinearities of other types, including saturable [28], quadratic (alias second-harmonic-generating) [29, 30], cubic-quintic (CQ) [31], and nonlocal cubic interactions [32]. Unlike the Kerr nonlinearity, more general types of the self-interaction of light can be realized not in fibers (i.e., not in the *temporal domain*), but rather in planar waveguides (i.e., in the *spatial domain*). Theoretical modeling of these settings is facilitated by the fact that the respective nonlinear Schrödinger equations (NLSEs) for the evolution of the local amplitude of the electromagnetic waves takes identical forms in the temporal and spatial domains, with the temporal variable replaced by the transverse spatial coordinate, in the latter case. Generally, dual-core systems are adequately modeled by systems of two linearly coupled NLSEs, in which the linear coupling represents the tunneling of electromagnetic fields between the cores [6, 33, 34].

Further, effective *discretization* of continuous nonlinear couplers may be provided, in the spatial domain too, by the consideration of parallel arrays of discrete waveguides [50]-[52]. The coupler concept was also extended for the *spatiotemporal* propagation of light in dual-core planar waveguides, with the one-dimensional (1D) NLSE replaced by its two-dimensional (2D) version, which includes both the temporal and spatial transverse coordinates [53].

Similar to the double-fiber waveguides for optical waves are dual-core cigar-shaped (strongly elongated) traps for matter waves in atomic Bose-Einstein condensates (BECs)

[54]. Transmission of matter waves in these settings have been studied theoretically [55–57], making use of the fact that the Gross-Pitaevskii equation (GPE) for the mean-field wave function of the matter waves in BEC [58] is actually identical to the NLSE for electromagnetic waves in similar optical waveguides.

The above-mentioned systems in optics and BEC imply lossless propagation of optical and atomic waves, hence the respective models are based on the NLSEs and GPEs which do not include dissipative terms. On the other hand, loss and gain play an important role in many optical systems, such as fiber lasers. The fundamental model of such systems is based on complex Ginzburg-Landau equations (CGLEs), i.e., an extension of the NLSE with real coefficients replaced by their complex counterparts [59, 60]. Accordingly, dual-core fiber lasers are described by systems of linearly coupled CGLEs [61]. Dissipative linearly coupled systems with the gain and loss applied to different cores are relevant too, as models admitting stable transmission [62–64], filtering [65], and nonlinear amplification [66] of optical pulses in fiber lasers with the cubic nonlinearity, see a brief review of the topic in [67].

A special system is one with exactly equal gain and loss acting in the parallel-coupled cores, which are identical as concerns other coefficients [68]. Such settings feature the \mathcal{PT} (parity-time) symmetry between the cores (for the general concept of the \mathcal{PT} symmetry, see original works [70]–[77] and reviews [78]–[81]). The linear spectrum of the \mathcal{PT} -symmetric coupler may remain purely real (i.e., it does not produce decay due to imbalanced loss or blowup due to imbalanced gain), provided that the gain-loss coefficient does not exceed a critical value (in fact, it is exactly equal to the coefficient of the linear coupling between the cores [68, 69]; see Section III below). Overall, \mathcal{PT} -symmetric settings may be considered as dissipative systems which are able to emulate conservative ones, as they support not only real spectra but also stable soliton families if appropriate nonlinearity is included [74, 80, 81], as is shown in detail below in Section III (generic dissipative systems create isolated nonlinear states (in particular, dissipative solitons [82]), which play the role of attractors, rather than continuous families of stable solutions).

Thus, nonlinear dual-core systems represent a vast class of settings relevant to optics, BEC, and other areas, which offer a possibility to model and predict many physically significant effects. As examples of similar systems which are well known in completely different areas of physics, it is relevant to mention tunnel-coupled pairs of long Josephson junction, which are described by systems of linearly coupled sine-Gordon equations (see original works

[83]-[85] and reviews [86, 87]), and the propagation of internal waves in stratified liquids with two well-separated interfaces, which are described by pairs of linearly-coupled Korteweg de Vries equations, which were derived in various forms [88]-[92]. The purpose of this article is to present a reasonably compact review of the corresponding models and results. Because the general topic is very broad, the review is limited to optical waveguides based on dual-core optical fibers. Related settings, such as those based on double planar waveguides and double traps for matter waves in BEC, are briefly mentioned in passing.

A fundamental property of nonlinear couplers with symmetric cores is the *symmetry-breaking bifurcation* (SBB), which destabilizes obvious symmetric modes (sometimes called *supermodes*, as they extend to both individual cores, which support individual modes), and gives rise to asymmetric states. The SBB was theoretically analyzed in detail for temporally uniform states (alias *continuous waves*, CWs) in dual-core nonlinear optical fibers [33], and, in parallel, for self-trapped solitary waves, i.e., temporal solitons in the same system [34]-[43], as well as for dual-core nonlinear fibers with Bragg gratings (BGs) written on each core [25]. Some results obtained in this direction were summarized in early review [48], and later in [49]. The SBB analysis was then extended to solitons in couplers with the quadratic [29] and CQ [31] nonlinearities.

The Kerr nonlinearity in the dual-core system gives rise to the *subcritical* SBB for solitons, with originally unstable branches of emerging asymmetric modes going backward (in the direction of weaker nonlinearity) and then turning forward [93]. The asymmetric modes retrieve their stability at the turning points. On the other hand, the *supercritical* SBB gives rise to stable branches of asymmetric solitons going in the forward direction. For solitons, the SBB of the latter type occurs in twin-core Bragg grating [25] (see subsection II.D below), and in the system with the quadratic nonlinearity [29]. The coupler with the intra-core CQ nonlinearity gives rise to a closed *bifurcation loop*, whose shape may be concave or convex [31] (see details in subsection II.E below).

In models of nonlinear dual-core couplers, the SBB point can be found in an exact analytical form for the system with the cubic nonlinearity [34], and the emerging asymmetric modes were studied by means of the variational approximation (VA) [12, 25, 28, 29, 35, 53] and numerical calculations [38, 39], see also reviews [48] and [49].

In addition to the studies of solitons in uniform dual-core systems, the analysis was developed for *fused couplers*, in which the two cores are joined in a narrow segment [94].

In the simplest approximation, the corresponding dependence of the coupling strength on coordinate z may be approximated by the delta-function, $\delta(z)$. Originally, interactions of solitons with a locally fused segment were studied in the temporal domain, *viz.*, for bright [94–96] and dark [97] solitons in dual-core optical fibers and fiber lasers [98]. In that case, the coupling affects the solitons only in the course of a short interval of their evolution. The *spatial-domain* optical counterpart of the fused coupler is provided by a dual-core planar waveguide with a narrow coupling segment created along the coordinate (x) perpendicular to the propagation direction (z) [99, 100]. Dynamics of spatial optical solitons in such settings, including stationary solitons trapped by the fused segment of the coupler, and scattering of incident solitons on one or several segments, was analyzed in [101].

The objective of this article is to present a review of basic findings produced by studies of models developed for dual-core nonlinear optical fibers and fiber lasers, along the above-mentioned directions. The review is chiefly focused on theoretical results, as experimental ones are still missing for solitons, in most cases. In Section II, the most fundamental results are summarized for the SBBs of solitons in dual-core fibers with identical cores. Some essential findings for asymmetric waveguides, with different cores, are included too. The results are produced by a combination of numerical and methods and analytical approximations (primarily, the variational approximation, VA). In Section III, the results are presented for the creation of stable dissipative solitons in models of fiber lasers, the stabilization being provided by coupling the main core, which carries the linear gain, to a parallel lossy one. Section IV is focused on nonlinear dual-core couples featuring the above-mentioned parity-time (\mathcal{PT}) symmetry, which is provided by creating mutually balanced gain and loss in two otherwise identical cores, the main issue being stability conditions for the corresponding \mathcal{PT} -symmetric solitons (which can be solved in an exact analytical form, in this model). The article is concluded by Section V.

II. SOLITONS IN DUAL-CORE FIBERS

A. The symmetry-breaking bifurcation (SBB) of solitons

1. The formulation of the model

The basic model of the symmetric coupler, i.e., a dual-core fiber with equal dispersion and nonlinearity coefficients in the parallel-coupled cores, is represented by a system of linearly coupled NLSEs, which are written here in the scaled form [3], with subscripts standing for partial derivatives:

$$iu_z + \frac{1}{2}u_{\tau\tau} + |u|^2u + Kv = 0, \quad (1)$$

$$iv_z + \frac{1}{2}v_{\tau\tau} + |v|^2v + Ku = 0, \quad (2)$$

where z is the propagation distance, $\tau \equiv t - z/V_{\text{gr}}$ is the reduced time (t is the physical time, and V_{gr} is the group velocity of the carrier wave [102]), u and v are amplitudes of the electromagnetic waves in the two cores, sign $+$ in front of the group-velocity-dispersion (GVD) terms, represented by the second derivatives, implies the anomalous character of the GVD in the fiber [102], the cubic terms represent the intra-core Kerr effect, and K , which is defined to be positive (actually, it may be scaled to $K \equiv 1$) is the coupling constant accounting for the light exchange between the cores.

An additional effect which can be included in the model represents the temporal dispersion of the inter-core coupling, represented by its own real coefficient, K' . The accordingly modified Eqs. (1) and (2) take the form [42]

$$iu_z + \frac{1}{2}u_{\tau\tau} + |u|^2u + Kv + iK'v_{\tau} = 0, \quad (3)$$

$$iv_z + \frac{1}{2}v_{\tau\tau} + |v|^2v + iKu + K'u_{\tau} = 0. \quad (4)$$

Below, this generalization of the nonlinear-coupler model is not considered in detail, as detailed analysis has demonstrated that the dispersion of the inter-core coupling does not produce drastic changes in properties of solitons [103].

Equations (1) and (2) can be derived, by means of the standard variational procedure, from the respective Lagrangian (L), which, in turns, includes the Hamiltonian of the system

(H) [49]:

$$L = \int_{-\infty}^{+\infty} \left[\frac{i}{2} (u^* u_z + v^* v_z) d\tau + \text{c.c.} \right] - H, \quad (5)$$

$$H = \int_{-\infty}^{+\infty} \left[\frac{1}{2} (|u_\tau|^2 + |v_\tau|^2) - \frac{1}{2} (|u|^4 + |v|^4) - K (u^* v + uv^*) \right], \quad (6)$$

where both * and c.c. stand for the complex-conjugate expressions. The Hamiltonian, along with the integral energy (alias total norm) of the solution,

$$E = \frac{1}{2} \int_{-\infty}^{+\infty} (|u|^2 + |v|^2) d\tau, \quad (7)$$

and the total momentum,

$$P = \frac{i}{2} \int_{-\infty}^{+\infty} [(u u_\tau^* + v v_\tau^*) + \text{c.c.}] d\tau, \quad (8)$$

are dynamical invariants (conserved quantities) of the system.

If the dispersion of the inter-core dispersion is included, see Eqs. (3) and (4), the additional term in the Hamiltonian density in Eq. (6) is $-(iK/2)(u^* v_\tau + v^* u_\tau - uv_\tau^* - vu_\tau^*)$, while the expression for the total energy and momentum keep the same form as defined in Eqs. (7) and (8).

Equations (1) and (2) admit obvious symmetric and antisymmetric soliton solutions (*supermodes*),

$$u = \pm v = a^{-1} \text{sech} \left(\frac{\tau}{a} \right) \exp \left(\frac{iz}{2a^2} \pm iKz \right), \quad (9)$$

where a is an arbitrary width, which determines the total energy (7) and Hamiltonian (6) of the symmetric and antisymmetric states:

$$E_{\text{symm-sol}} = 2a^{-1}, \quad H_{\text{symm-sol}} = -\frac{2}{3}a^{-3} \mp 4Ka^{-1}. \quad (10)$$

In the case of $K > 0$ (that may always be fixed by definition), the antisymmetric solitons are unstable [39], as they correspond to a maximum, rather than minimum, of the coupling term ($\sim K$) in Hamiltonian (10), therefore they are not considered below. For the symmetric solitons, the SBB, which destabilizes them and replaces them by stable asymmetric solitons, with different energies in the two cores, is an issue of major interest. The onset of the SBB of the symmetric soliton, i.e., the value of the soliton's energy at the SBB point, can be found in an exact analytical form [34]. To this end, one looks for a general (possibly asymmetric) stationary solution of Eqs. (1) and (2) for solitons with propagation constant k as

$$\{u(z, \tau), v(z, \tau)\} = e^{ikz} \{U(\tau), V(\tau)\}, \quad (11)$$

where real functions U and V satisfy the following ordinary differential equations:

$$\frac{1}{2} \frac{d^2 U}{d\tau^2} + U^3 + KV = kU, \quad (12)$$

$$\frac{1}{2} \frac{d^2 V}{d\tau^2} + V^3 + KU = kV. \quad (13)$$

The SBB corresponds to the emergence of an *antisymmetric* eigenmode of infinitesimal perturbations,

$$\{\delta U(\tau), \delta V(\tau)\} = \varepsilon \{U_1(\tau), -U_1(\tau)\} \quad (14)$$

(ε is a vanishingly small perturbation amplitude) around the unperturbed symmetric solution of Eqs. (12) and (13), which is taken as per Eq. (9), i.e.,

$$U_0(\tau) = V_0(\tau) \equiv a^{-1} \operatorname{sech}\left(\frac{\tau}{a}\right), \quad k = \frac{1}{2a^2} + K. \quad (15)$$

The linearization of Eqs. (12) and (13) around the exact symmetric state leads to the equation

$$\frac{1}{2} \frac{d^2 U_1}{d\tau^2} + 3U_0^2 U_1 - (K + k) U_1 = 0, \quad (16)$$

which is tantamount to the stationary version of the solvable 1D linear Schrödinger equation with the Pöschl-Teller potential. Then, with the help of well-known results from quantum mechanics [104], it is easy to find that, with the growth of the soliton's energy E , i.e., with the increase of k (see Eqs. (10) and (15)), a nontrivial eigenstate, produced by Eq. (16), appears at [34]

$$E = E_{\text{bif}} \equiv 4\sqrt{K/3} \approx 2.31\sqrt{K}. \quad (17)$$

Thus, the SBB and destabilization of the symmetric solitons (15) take place precisely at point (17).

2. Continuous-wave (CW) states and their modulational instability (MI)

To complete the formulation of the model of the symmetric nonlinear coupler, it is relevant to mention that, besides the solitons, it admits simple continuous-wave (CW) states, with constant U and V in Eq. (11). Indeed, Eqs. (12) and (13) easily produce the full set of CW solutions: symmetric and antisymmetric ones,

$$U_{\text{symm}}^{(\text{CW})} = V_{\text{symm}}^{(\text{CW})} = \sqrt{k - K}, \quad U_{\text{anti}}^{(\text{CW})} = -V_{\text{anti}}^{(\text{CW})} = \sqrt{k + K}, \quad (18)$$

which exist, respectively, at $k > K$ and $k > -K$, respectively. With the growth of k , i.e., increase of the CW amplitude, the symmetric state undergoes the SBB at $k = 2K$, giving rise to asymmetric CW states, which exist at $k > 2K$:

$$U_{\text{asymm}}^{(\text{CW})} = \sqrt{\frac{k}{2} + \sqrt{\frac{k^2}{4} - K^2}}, \quad V_{\text{asymm}}^{(\text{CW})} = \sqrt{\frac{k}{2} - \sqrt{\frac{k^2}{4} - K^2}} \quad (19)$$

(and its mirror image, with $U \rightleftharpoons V$). The SBB for CW states in models of couplers with more general nonlinearities was studied in detail in Ref. [33].

However, all the CW states are subject to the *modulational instability* (MI) [40], which, roughly speaking, tends to split the CW into a chain of solitons. While this conclusion is not surprising in the case of the anomalous GVD in Eqs. (1) and (2), as it gives rise to the commonly known MI in the framework of the single NLSE [102], all symmetric and asymmetric CW states are modulationally unstable too in the system of linearly coupled NLSEs with the normal sign of the GVD in each equation [41], this MI being produced by the linear coupling. Because of the instability of the CW background, nonlinear couplers, even with normal GVD, cannot support stable dark solitons or domain walls, i.e., delocalized states in the form of two semi-infinite asymmetric CWs, which are transformed into each other by substitution $U \rightleftharpoons V$, linked by a transient layer [44]. Because bright solitons cannot exist in the case of the normal GVD, the development of the MI in the latter case leads to a state in the form of “optical turbulent” [41].

As concerns the temporal dispersion of the inter-core coupling (see Eqs. (3) and (4)), its effect on the MI of the CW states was studied in Ref. [45].

3. The variational approximation (VA) for solitons

Asymmetric solitons, which emerge at the SBB point, cannot be found in an exact form, but they can be studied by means of the VA. This approach for solitons in nonlinear couplers was developed in works [35]-[37], see also work [105] which discussed limitations of the VA in this setting. Here, the main findings produced by the VA, and their comparison with results obtained by means of numerical methods are presented as per work [43].

The VA is based on the following trial analytical form (*ansatz*) for the two-soliton soliton:

$$u = A \cos(\theta) \operatorname{sech}\left(\frac{\tau}{a}\right) \exp(i(\phi + \psi) + ib\tau^2), \quad (20)$$

$$v = A \sin(\theta) \operatorname{sech}\left(\frac{\tau}{a}\right) \exp(i(\phi - \psi) + ib\tau^2). \quad (21)$$

where real variational parameters, A , θ , a , ϕ , ψ , b , may be functions of the propagation distance, z . In particular, $A(z)$ and $a(z)$ are common amplitude and width of the two components, chirp $b(z)$ must be introduced, as it is well known [46, 47], in the dynamical ansatz which allows evolution of the soliton's width, $\phi(z)$ is an overall phase of the two-component soliton, angle $\theta(z)$ accounts for the distribution of the energy between the components, and $\psi(z)$ is a relative phase between them. The shape and phase parameters form conjugate pairs, *viz.*, (A, ϕ) , (θ, ψ) , and (a, b) .

Note that the ansatz based on Eqs. (20) and (21) assumes that centers of the two components of the soliton are stuck together. This implies that the linear coupling between the two cores is strong, which corresponds to the real physical situation. Nevertheless, it is also possible to consider a case when the linear coupling plays the role of a small perturbation, making a two-component soliton a weakly bound state of two individual NLSE solitons belonging to the two cores [106–108].

Switching of a soliton between the two cores of the coupler was considered, on the basis of a full system of variational equations for ansatz (20), (21) in work [109]. It was also demonstrated in work [110] that the approximation for the switching dynamics in the nonlinear coupler can be further improved if the radiation component of the wave field is incorporated into the ansatz.

Here, the consideration is focused on the basic case of static solitons, for which ansatz (20), (21) gives rise to the following variational equations, in which all parameters of ansatz (20)-(21), but overall phase ϕ , are assumed constant:

$$\sin(2\theta) \sin(2\psi) = 0, \quad (22)$$

$$\frac{E}{3a} \cos(2\theta) - K \cot(2\theta) \cos(2\psi) = 0, \quad (23)$$

$$a^{-1} = E \left[1 - \frac{1}{2} \sin^2(2\theta) \right], \quad (24)$$

$$\frac{d\phi}{dz} = -\frac{1}{6a^2} + \frac{2E}{3a} \left(1 - \frac{1}{2} \sin^2(2\theta) \right) + \kappa \sin(2\theta) \cos(2\psi),$$

where E is the soliton's energy, which, according to its definition (7), takes value $E = A^2 a$ for ansatz (20), (21).

As it follows from Eq. (22), the static soliton may have either $\sin(2\theta) = 0$, or $\sin(2\psi) = 0$. According to the underlying ansatz, the former solution implies that all the energy resides in a single core, which contradicts Eqs. (1) and (2), hence this solution is spurious. The latter solution, $\sin(2\psi) = 0$, implies that $\cos(2\psi) = \pm 1$. As mentioned above, the solutions corresponding to $\cos(2\psi) = -1$, i.e., antisymmetric ones, with respect to the two components, are unstable. Therefore, only the case of $\cos(2\psi) = +1$, corresponding to solitons with in-phase components, is considered here. Then, width a can be eliminated by means of Eq. (24), and the remaining equation (24) for the energy-distribution angle θ takes the form of

$$\cos(2\theta) \left[\frac{E^2}{3K} \sin(2\theta) \left(1 - \frac{1}{2} \sin^2(2\theta) \right) - 1 \right] = 0. \quad (25)$$

Further analysis reveals that, in the interval $0 < E^2 < E_1^2$, where

$$E_1^2 = (9/4)\sqrt{6}K \approx 5.511 K, \quad (26)$$

the only relevant solution to Eq. (25) is the symmetric one, with $\theta = \pi/4$ (corresponding to $\cos(2\theta) = 0$) and equal energies in both components, according to Eqs. (20) and (21). When the soliton's energy attains value E_1 , predicted by Eq. (26), there emerge *asymmetric* solutions with $\cos(2\theta) = \pm 1/\sqrt{3}$. When E^2 attains a slightly larger value,

$$E_2^2 = 6K, \quad (27)$$

a *backward (subcritical) bifurcation* [93] occurs, which makes the symmetric solution with $\theta = \pi/4$ unstable. The comparison with full numerical results corroborates the weakly subcritical shape of the SBB for solitons in the nonlinear coupler.

A typical example of an asymmetric soliton is displayed in Fig. 1, and the entire bifurcation diagram is presented in Fig. 2. Note that quantity $\cos(2\theta)$, which is used as the vertical coordinate in the diagram, measures the asymmetry of the soliton, because, as it follows from Eqs. (20) and (21),

$$\cos(2\theta) \equiv \frac{E^{(1)} - E^{(2)}}{E^{(1)} + E^{(2)}}, \quad (28)$$

where $E^{(j)}$ is the energy in the j -th core. Even without detailed stability analysis, one can easily distinguish between stable and unstable branches in the diagram, using elementary theorems of the bifurcation theory [93].

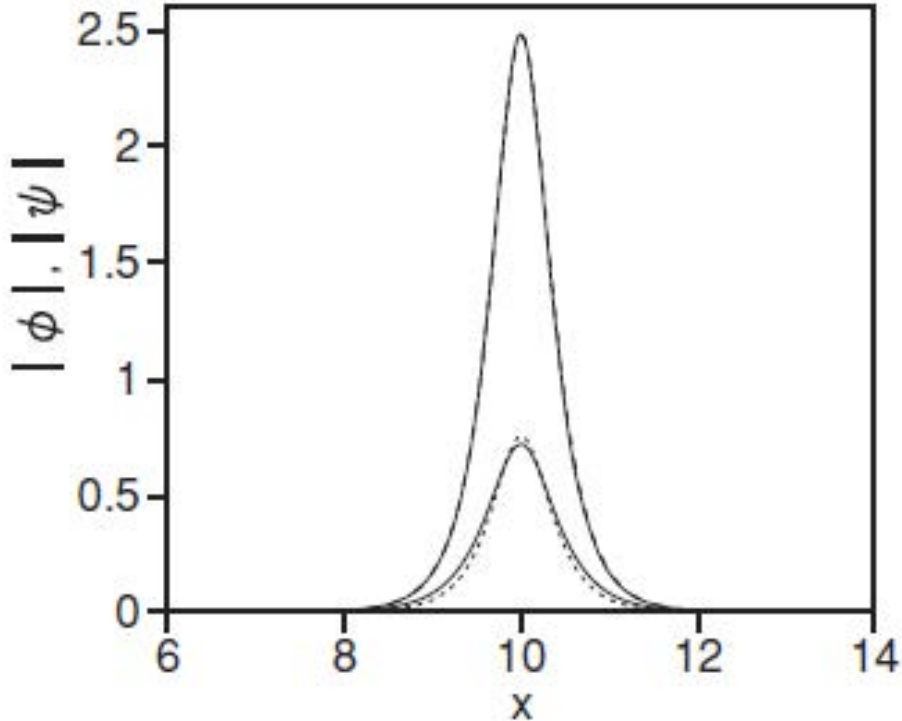


FIG. 1: A typical example of two components of a stable asymmetric soliton, with $|\phi(x)| \equiv U(\tau)$, $|\psi(x)| \equiv V(\tau)$, as per Ref. [111]. Continuous and dashed lines designate the numerically found solution and its VA-produced counterpart, respectively.

Thus, the VA predicts the backward bifurcation at the soliton's energy $E_2 = \sqrt{6K} \approx 2.45\sqrt{K}$. The accuracy of the VA is characterized by comparison of this prediction with the above-mentioned exactly found bifurcation value (17), the relative error being 0.057 (the analytical solutions for E_{bif} does not predict the subcritical character of the SBB).

The above consideration addressed a single soliton in the nonlinear coupler. A cruder version of the VA was used in work [112] to analyze two-soliton interactions in the same system. Accurate numerical results for the interaction were reported in [114]. Furthermore, it was recently demonstrated that chains of stable solitons with opposite signs between adjacent ones, in the dual-core fiber, support the propagation of *supersolitons*, i.e., self-trapped collective excitations in the chain of solitons [113]. The underlying chain may be built of symmetric solitons, as well as of asymmetric ones, with alternating polarities, i.e., placements of larger and smaller components in the two cores.

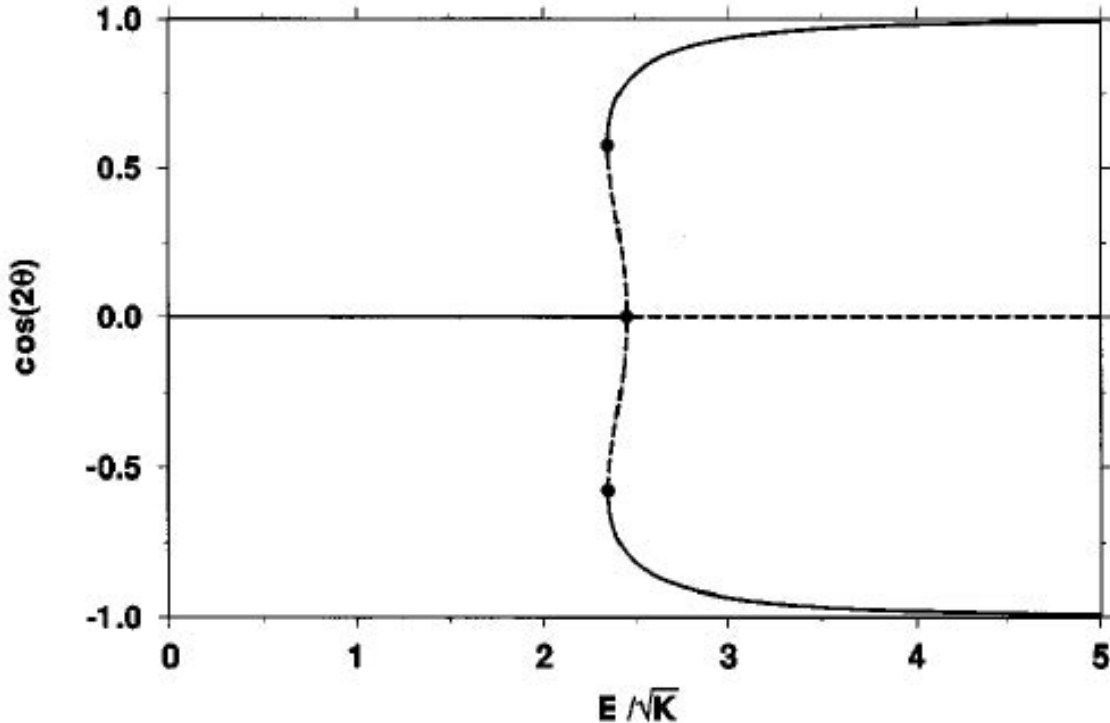


FIG. 2: The dependence of the asymmetry parameter of two-component solitons in the nonlinear coupler with identical cores, $\cos(2\theta)$, on the scaled total energy, E/\sqrt{K} , as predicted by the VA, see Eq. (28). The figure demonstrates a weakly subcritical SBB, solid and dashed lines designating stable and unstable states, respectively. The results are presented as per Ref. [43].

B. Gap solitons in asymmetric dual-core fibers

Asymmetric dual-core fibers, consisting of two different cores, can be easily fabricated, and properties of solitons in them may be markedly different from those in the symmetric couplers. A general model of the asymmetric coupler is (cf. Eqs. (1), (2))

$$iu_z + qu + \frac{1}{2}u_{\tau\tau} + |u|^2u + v = 0, \quad (29)$$

$$iv_z - \delta \cdot \left(qv + \frac{1}{2}v_{\tau\tau} \right) + |v|^2v + u = 0, \quad (30)$$

where real parameter $-\delta$ accounts for the difference between GVD coefficients in the cores, and another real coefficient, $(1 + \delta)q$, defines the phase-velocity mismatch between them, while a possible group-velocity mismatch can be eliminated in the equations by a simple transformation.

The effect of the asymmetry between the cores on the SBB for solitons was addressed in Refs. [43] and [115] (strictly speaking, in this case the subject of the analysis is spontaneous breaking of *quasi-symmetry*, which remains after lifting the exact symmetry by the mismatch between the cores). In [115], a VA-based analytical approach was elaborated, which showed good agreement with numerical results. A noteworthy feature of the SBB in the asymmetric model is a possibility of hysteresis in a broad region, while in the symmetric system the hysteresis occurs in the narrow bistability region between the two bifurcation points, as seen in Fig. 2. A systematic analysis of the MI of CW states in the model of asymmetric nonlinear couplers was reported in Ref. [116].

The most interesting version of the asymmetric model is one with $\delta > 0$ in Eq. (30), i.e., with *opposite* signs of the GVD [117]. In this case, the substitution of $u, v \sim \exp(ikz - i\omega\tau)$ in the linearized version of Eqs. (29) and (30) yields the respective dispersion relation,

$$k = \frac{1}{4}(\delta - 1)(\omega^2 - 2q) \pm \sqrt{\frac{1}{16}(\delta + 1)^2(\omega^2 - 2q)^2 + 1}. \quad (31)$$

Self-trapped states may exist, as *gap solitons* (GSs), at values of the propagation constant, k , that belong to the *gap* in spectrum (31), i.e., such that values of ω corresponding to given k , as per Eq. (31), are unphysical (imaginary or complex). The gap always exists in the case of $\delta > 0$, as seen from typical examples of the spectra for negative and positive mismatch q , which are displayed in Fig. 3. If the formal values of ω in the gap are complex, GS's tails decay with oscillations, while for pure imaginary ω they decay monotonously. In particular, it follows from Eq. (31) that, in subgap $0 \leq k^2 < 4\delta/(1 + \delta)^2$, the tails always decay with oscillations.

Solutions to Eqs. (29) and (30) for stationary GSs are sought for as $u(z, \tau) = U(\tau) \exp(ikz)$, $v(z, \tau) = V(\tau) \exp(ikz)$, with real U and V determined by equations

$$\begin{aligned} (q - k)U + \frac{1}{2} \frac{d^2U}{d\tau^2} + U^3 + V &= 0, \\ -(\delta q + k)V - \frac{1}{2} \delta \frac{d^2V}{d\tau^2} + V^3 + U &= 0. \end{aligned} \quad (32)$$

Approximate solutions to Eqs. (32) can be constructed by means of the VA, using the Gaussian ansatz

$$U = A \exp(-\tau^2/2a^2), \quad V = B \exp(-\tau^2/2b^2). \quad (33)$$

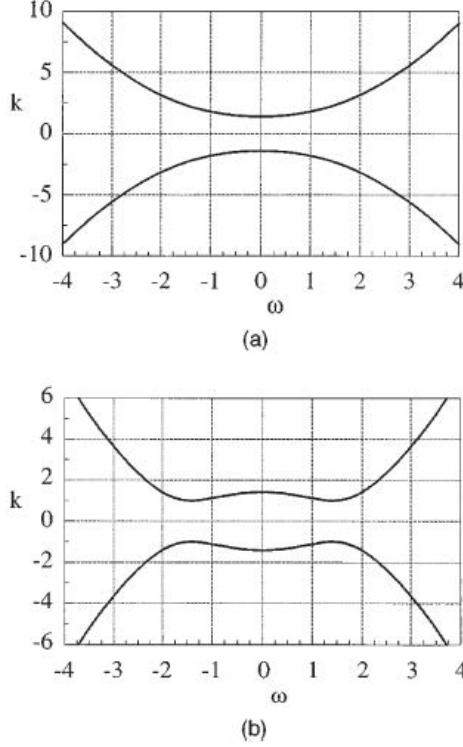


FIG. 3: Typical dispersion curves produced by Eq. (31) for the dual-core fiber with opposite signs of the GVD in the cores, corresponding to Eqs. (29) and (30) with $\delta = 1$: (a) $q = -1$; (b) $q = +1$ (as per Ref. [117]).

Energies of the two components of the soliton corresponding to this ansatz are

$$E_u \equiv \int_{-\infty}^{+\infty} |U(\tau)|^2 dt = \sqrt{\pi} A^2 a, \quad E_v \equiv \int_{-\infty}^{+\infty} |V(\tau)|^2 dt = \sqrt{\pi} B^2 b, \quad (34)$$

with the net energy $E \equiv E_u + E_v$.

Elimination of amplitudes A and B from the resulting system of variational equations leads to coupled equations for the widths a and b ,

$$[3 - 4(k - q)a^2] [3\delta + 4(k + \delta q)b^2] = 32(ab)^3 (b^2 - 3a^2) (3b^2 - a^2) (a^2 + b^2)^{-3}, \quad (35)$$

$$\frac{[3 - 4(k - q)a^2] (3a^2 - b^2)^2}{[3\delta + 4(k + \delta q)b^2] (3b^2 - a^2)^2} = \frac{a^3 [\delta (3a^2 + b^2) + 4(k + \delta q)b^2 (b^2 - a^2)]}{b^3 [(3b^2 + a^2) + 4(k - q)a^2 (b^2 - a^2)]}. \quad (36)$$

These equations can be solved numerically, to find a and b as functions of propagation constant k and parameters δ and q .

The results reported in [117] demonstrate that the GSs indeed exist in a part of the available gap, and, in most cases, they are stable. However, another part of the gap remains

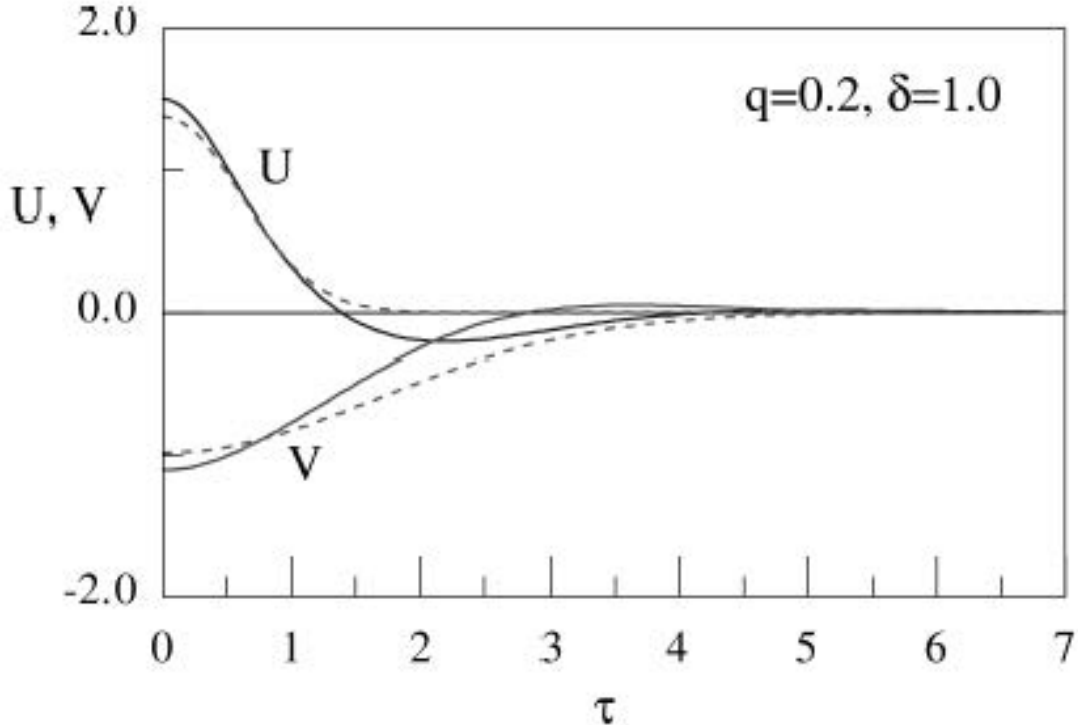


FIG. 4: A numerically found (solid lines) gap-soliton solution of Eqs. (29) and (30) with oscillating decaying tails, and its VA-predicted counterpart (dashed lines), in the case of $\delta = 1$ (opposite GVD in the two cores) and $q = 0.2$. The total energy of the numerically found gap soliton is $E = 2.734$ (as per Ref. [117]).

empty (there are intervals of k in the gap where no soliton can be found). A noteworthy feature of the GSs is that more than half of their net energy *always* resides in the normal-GVD component v , in spite of the obvious fact that the normal-GVD core cannot, by itself, support any bright soliton. Further, a typical GS predicted by the VA (see Fig. 4) has a narrower component with a larger amplitude in the anomalous-GVD core, and a broader component with a smaller amplitude in the normal-GVD one, see Fig. 4.

As is seen from Fig. 4, the VA generally correctly approximates the soliton's core, but the simplest ansatz (33) does not take into regard the fact that, as it mentioned above, the soliton's tails decay with oscillations. The contribution of the tails also accounts for a conspicuous difference of the energy share E_v/E in the normal-GVD core from the value predicted by the VA for the same net energy E : for example, in the case shown in Fig. 4, the VA-predicted value is $E_v/E = 0.585$, while its numerically found counterpart is

$E_v/E = 0.516$ (but it exceeds $1/2$, as stressed above).

C. The coupler with separated nonlinearity and dispersion

For better understanding of the light dynamics in strongly asymmetric nonlinear couplers, it is relevant to consider the model of an extremely asymmetric dual-core waveguide, in which the Kerr nonlinearity is carried by one core, and the GVD is concentrated in the other [118]. Such a system, although looking “exotic”, can be created by means of available technologies, by adjusting the zero-dispersion point of the first core to the carrier wavelength of the optical signal, and using a large effective cross-section area in the first core to suppress its nonlinearity. The respective system of coupled equations is

$$iu_z + |u|^2u + v = 0, \quad (37)$$

$$iv_z + qv + (D/2)v_{\tau\tau} + u = 0, \quad (38)$$

cf. Eqs. (1) and (). Here the inter-core coupling coefficient is normalized to be 1, real parameter q , which may be positive or negative, is the phase-velocity mismatch between the cores, and D is the GVD coefficient, that we may be scaled to be $+1$ or -1 , which corresponds to the anomalous or normal GVD, respectively. Group-velocity terms, such as ic_1u_τ in Eq. (37) and ic_2v_τ in Eq. (38), with some real coefficients c_1 and c_2 , can be removed: the former one by the shift of the velocity of the references frame, $\tau \rightarrow \tau - c_1z$, and the latter one by the phase transformation, $v \rightarrow v \exp(ic_2\tau/D)$. Therefore, these terms are not included.

Looking for a solution to the linearized version of Eqs. (37) and (38) in the usual form, $\{u, v\} \sim \exp(ikx - i\omega\tau)$ with real ω , one arrives at the dispersion relation,

$$k = -\frac{1}{2} \left(\frac{1}{2}D\omega^2 - q \right) \pm \sqrt{\frac{1}{4} \left(\frac{1}{2}D\omega^2 - q \right)^2 + 1}. \quad (39)$$

Straightforward consideration of the spectrum defined by this expression demonstrates that, in the case of the anomalous GVD ($D = +1$), it gives rise to *finite* and *semi-infinite gaps*,

$$-\frac{1}{2} \left(\sqrt{4 + q^2} - q \right) < k < 0; \quad \frac{1}{2} \left(\sqrt{4 + q^2} + q \right) < k < \infty, \quad (40)$$

and in the case of the normal GVD ($D = -1$), the *semi-infinite* and *finite gaps* are

$$-\infty < k < \frac{1}{2} \left(\sqrt{4 + q^2} - q \right); \quad 0 < k < \frac{1}{2} \left(\sqrt{4 + q^2} + q \right). \quad (41)$$

Note that both gaps (40) are broader than their counterparts (41) at $q > 0$, and vice versa at $q < 0$.

Equation (39) can be inverted, to yield $\omega^2 = 2(Dk)^{-1}(1 + qk - k^2)$. This relation implies that, inside both the finite and semi-infinite gaps, ω^2 takes real negative values, suggesting a possibility to find exponentially localized solitons in both gaps. To realize this possibility, soliton solutions of Eqs. (37) and (38) were looked for as $\{u, v\} = \exp(ikz) \{U(\tau), V(\tau)\}$. In the case of anomalous GVD, $D = +1$, it was thus found that the semi-infinite gap is *completely filled* by *stable* solitons, while the finite bandgap remains completely empty. This result does not depend on the magnitude and sign of the mismatch parameter, q , in Eq. (38). A typical example of the stable solitons found in the semi-infinite gap is shown in Fig. 5. Naturally, the shape of the soliton in the dispersive mode (V) is much smoother than in the nonlinear one (U). Nevertheless, the shapes of both components are strictly smooth; in particular, there is no true cusp at the tip of the dispersive one.

The fact that the anomalous GVD supports stable solitons in the semi-infinite gap of the present system is not surprising, as the situation seems qualitatively similar to what is commonly known for the usual NLSE, even if the shape of the solitons is very different from that in the NLSE, see Fig. 5. More unexpected is the situation in the case of the normal GVD, $D = -1$ in Eq. (38). As found in Ref. [118], in this case the semi-infinite gap remains empty, but the *finite* one is *completely filled* by *stable GSs*, see a typical example in Fig. 6.

It is relevant to mention that Eqs. (37) and (38) are not Galilean invariant. In accordance with this, it was not possible to create moving solitons in the framework of this system.

The analysis was also extended for the case when the nonlinear mode has weak residual GVD, of either sign [118]. Still earlier, a similar model was considered in Ref. [119], which introduced a two-core system with the nonlinearity in one core, and a linear BG in the other. That system creates a rather complex spectral structure, featuring three bandgaps, and a complex family of soliton solutions, including the so-called *embedded* solitons, which, under special conditions, may exist in (be *embedded into*) spectral bands filled by linear waves, where, generically, solitons cannot exist [120].

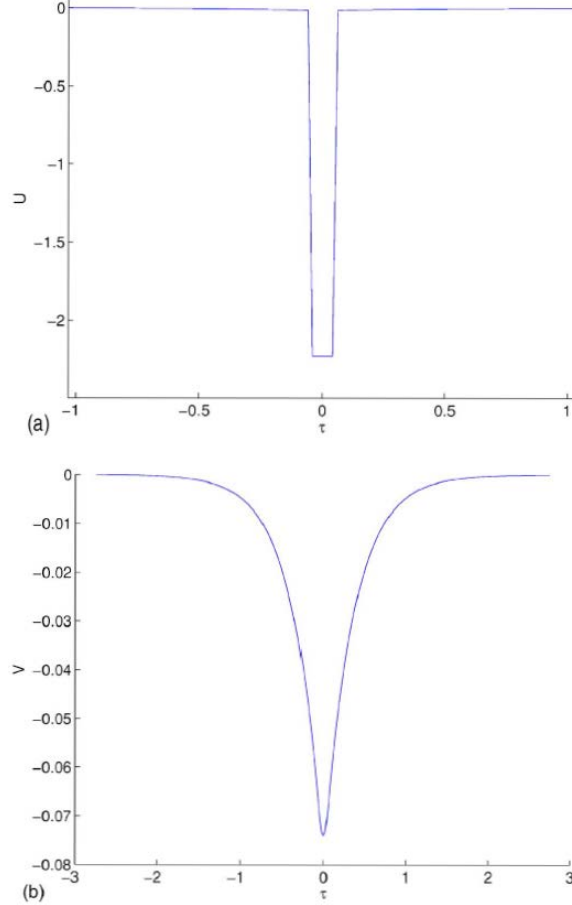


FIG. 5: An example of a stable soliton generated by the two-core system with separated nonlinearity and dispersion, based on Eqs. (37) and (38), with parameters $D = 1$ (the anomalous sign of the GVD) and mismatch $q = 0.8$. The propagation constant corresponding to this soliton is $k = 5$, which places it in the semi-infinite gap, see Eq. (40). Panels (a) and (b) display, respectively, the nonlinear- and dispersive-mode components of the soliton.

D. Two polarizations of light in the dual-core fiber

A relevant extension of the model of the nonlinear coupler takes into regard two linear polarizations of light in each core. In this case, Eqs. (29) and (30) are replaced by a system

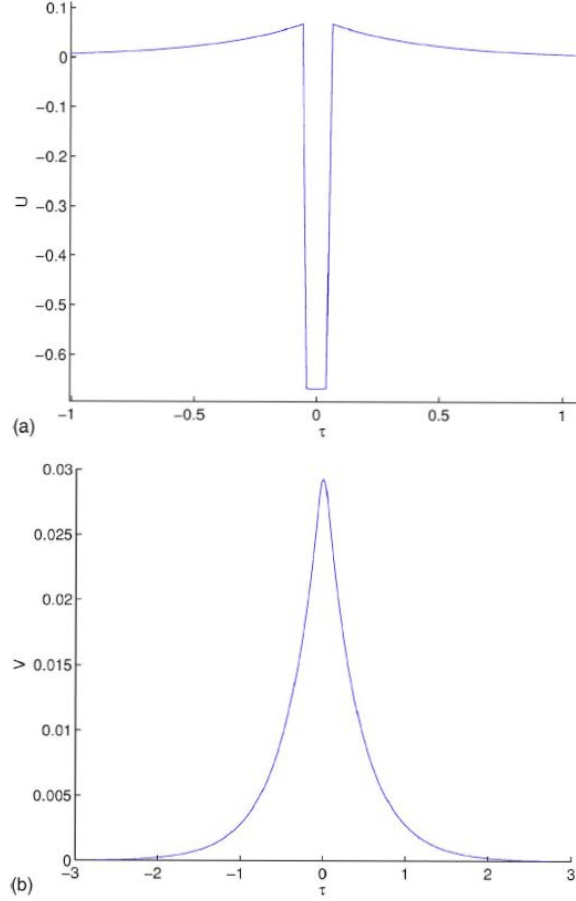


FIG. 6: The same as in Fig. 5, but for parameters $D = -1$ (the normal sign of the GVD) and mismatch $q = 0.8$. The propagation constant of this stable soliton is $k = 0.4$, placing it in the finite bandgap, see Eq. (41).

of four equations,

$$\begin{aligned}
 i(u_1)_z + \frac{1}{2}(u_1)_{\tau\tau} + (|u_1|^2 + \frac{2}{3}|v_1|^2)u_1 + u_2 &= 0, \\
 i(v_1)_z + \frac{1}{2}(v_1)_{\tau\tau} + (|v_1|^2 + \frac{2}{3}|u_1|^2)v_1 + v_2 &= 0, \\
 i(u_2)_z + \frac{1}{2}(u_2)_{\tau\tau} + (|u_2|^2 + \frac{2}{3}|v_2|^2)u_2 + u_1 &= 0, \\
 i(v_2)_z + \frac{1}{2}(v_2)_{\tau\tau} + (|v_2|^2 + \frac{2}{3}|u_2|^2)v_2 + v_1 &= 0,
 \end{aligned} \tag{42}$$

where fields u and v represent the two linear polarizations, the subscripts 1 and 2 label the cores, and the coupling coefficient is scaled to be $K \equiv 1$. In the case of circular polarizations (rather than linear ones), the XPM (cross-phase-modulation) coefficient $2/3$ in Eq. (42) is replaced by 2.

Four-component soliton solutions to Eqs. (42) can be looked for by means of the VA based on the Gaussian ansatz,

$$u_{1,2}(z, \tau) = A_{1,2} \exp(ipz - a^2\tau^2/2), \quad v_{1,2}(z, \tau) = B_{1,2} \exp(iqz - b^2\tau^2/2), \quad (43)$$

with mutually independent real propagation constants p and q . Existence regions for all the solutions in the (p, q) plane, produced by the VA for symmetric and asymmetric solitons (the asymmetry is again realized with respect to the two mutually symmetric cores) are displayed in Fig. 7, in the most essential case when the signs of amplitudes $A_{1,2}$ and $B_{1,2}$ in each polarization coincide (otherwise, all the solitons are unstable). Outside the shaded area in Fig. 7, there exist only solutions with a single polarization (i.e., with either $v_{1,2} = 0$ or $u_{1,2} = 0$), which were considered above. In particular, at the dashed-dotted borders of the shaded area, asymmetric four-component solitons (denoted by symbol AS1 in Fig. 7) carry over into the two-component asymmetric solitons of the single-polarization system. The symmetric solitons exist inside the sector bounded by straight continuous lines. The SBB, which gives rise to the asymmetric solitons AS1 and destabilizes the symmetric ones, takes place along the short-dashed curve in the left lower corner of the shaded area.

There is an additional asymmetric soliton (AS2 in Fig. 7) in the inner area confined by the dashed curve. Thus, the total number of soliton solutions changes, as one crosses the bifurcation curves in Fig. 7 from left to right, from 1 to 3 to 5. However, soliton AS2 is generated from the symmetric one by an additional SBB, which takes place *after* the symmetric soliton has already been destabilized by the bifurcation that gives rise to asymmetric soliton AS1. For this reason, soliton AS2 is always unstable, while the primary asymmetric one AS1 is stable. Further details concerning the stability of different solitons in this model can be found in [122].

E. Solitons in linearly coupled fiber Bragg gratings (BGs)

In the systems described by the single or coupled NLSEs, the second-derivative terms account for the intrinsic GVD of the fiber or waveguide. On the contrary to this, strong *artificial dispersion* can be induced by a BG, i.e., a permanent periodic modulation of the refractive index written along the fiber (usually, the modulation is created in the fiber's cladding), the modulation period being equal to half the wavelength of the propagating

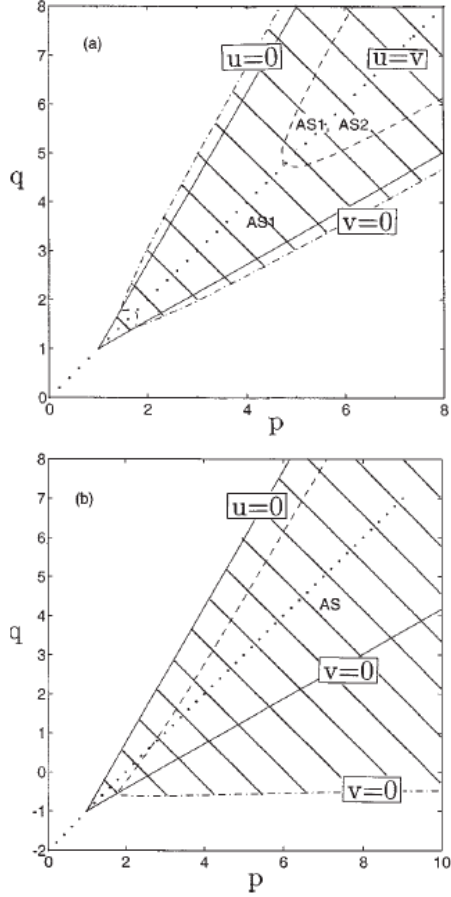


FIG. 7: Regions of existence of the symmetric and two types of asymmetric (stable, AS1, and unstable, AS2) solitons in the plane (p, q) of two propagation constants of four-component solitons (43), in the model (42) of the dual-core-fiber system carrying two linear polarizations of light. Symbols $u = 0$, $v = 0$, and $u = v$ refer to particular solutions with a single polarization and equal amplitudes of the two polarizations, respectively.

light. The nonlinear optical fiber carrying the BG is adequately described by the system of coupled-mode equations for amplitudes $u(x, t)$ and $v(x, t)$ of the right- and left-traveling waves [123, 124]:

$$iu_t + iu_x + [(1/2)|u|^2 + |v|^2]u + v = 0, \quad (44)$$

$$iv_t - iv_x + [|u|^2 + (1/2)|v|^2]v + u = 0. \quad (45)$$

Here, the speed of light in the fiber's material is scaled to be 1, as well as the linear-coupling constant, that accounts for mutual conversion of the right- and left traveling waves due to

the resonant reflection of light on the BG. The ratio of the XPM and SPM (self-phase-modulation) coefficients in Eqs. (44) and (45), 2 : 1, is the usual feature of the Kerr nonlinearity.

The dispersion relation of the linearized version of Eqs. (44) and (45) is $\omega^2 = 1 + k^2$, hence the existence of GSs (alias BG solitons) with frequencies belonging to the corresponding spectral bandgap, $-1 < \omega < +1$, may be expected. Indeed, although the system of Eqs. (44) and (45) is not integrable, it has a family of exact soliton solutions [125–127], which contains two nontrivial parameters, *viz.*, amplitude Q , which takes values $0 < Q < \pi$, and velocity c , which belongs to interval $-1 < c < +1$. In particular, the solution for the quiescent solitons ($c = 0$) is

$$\begin{aligned} u &= \sqrt{2/3}(\sin Q) \operatorname{sech}\left(x \sin Q - \frac{1}{2}iQ\right) \cdot \exp(-it \cos Q), \\ v &= -\sqrt{2/3}(\sin Q) \operatorname{sech}\left(x \sin Q + \frac{1}{2}iQ\right) \cdot \exp(-it \cos Q), \end{aligned} \quad (46)$$

where frequencies $\omega_{\text{sol}} \equiv \cos Q$ precisely fill the entire gap, while Q varies between 0 and π . Stability of the BG solitons was investigated too, the result being that they are stable, roughly, in a half of the bandgap, namely, at $0 < Q < Q_{\text{cr}} \approx 1.01 \cdot (\pi/2)$ [128–130].

A natural generalization of the fiber BG is a system of two parallel-coupled cores with identical gratings written on both of them [25]. The respective system of four coupled equations can be cast in the following normalized form, cf. Eqs. (44), (45) for the single-core BG fiber, and Eqs. (1), (2) for the dual-core fiber without the BG:

$$iu_{1t} + iu_{1x} + \left(\frac{1}{2}|u_1|^2 + |v_1|^2\right)u_1 + v_1 + \lambda u_2 = 0, \quad (47)$$

$$iv_{1t} - iv_{1x} + \left(\frac{1}{2}|v_1|^2 + |u_1|^2\right)v_1 + u_1 + \lambda v_2 = 0, \quad (48)$$

$$iu_{2t} + iu_{2x} + \left(\frac{1}{2}|u_2|^2 + |v_2|^2\right)u_2 + v_2 + \lambda u_1 = 0, \quad (49)$$

$$iv_{2t} - iv_{2x} + \left(\frac{1}{2}|v_2|^2 + |u_2|^2\right)v_2 + u_2 + \lambda v_1 = 0, \quad (50)$$

where λ is the coefficient of the linear coupling between the two cores, which may be defined to be positive (unlike the models considered above, it is not possible to fix $\lambda = 1$ by means of rescaling, because the scaling freedom has been already used to fix the Bragg-reflection coefficient equal to 1). The same model applies to the spatial-domain propagation in two parallel-coupled planar waveguides which carry BGs in the form of a system of parallel cores, in which case t and x play the roles of the propagation distance and transverse coordinate, respectively, while the paraxial diffraction in the waveguides is neglected.

The dispersion relation for system (47)-(50) contains four branches (taking into regard that ω may have two opposite signs):

$$\omega^2 = \lambda^2 + 1 + k^2 \pm 2\lambda\sqrt{1 + k^2}. \quad (51)$$

This spectrum has no gap in the case of strong inter-core coupling, $\lambda > 1$. For the weaker coupling, with $\lambda < 1$, the bandgap exists:

$$-(1 - \lambda) < \omega < +(1 - \lambda). \quad (52)$$

To populate the bandgap, solutions for zero-velocity GSs are looked for as

$$u_{1,2} = \exp(-i\omega t) U_{1,2}(x), \quad v_{1,2} = \exp(-i\omega t) V_{1,2}(x), \quad (53)$$

where relation $V_{1,2} = -U_{1,2}^*$ may be imposed (in fact, the exact GS solutions (46) in the single-core BG are subject to the same constraint). Substituting this in Eqs. (47)-(50) leads to two coupled equations (instead of four):

$$\omega U_1 + i \frac{dU_1}{dx} + \frac{3}{2}|uU_1|^2 U_1 - U_1^* + \lambda U_2 = 0, \quad (54)$$

$$\omega U_2 + i \frac{dU_2}{dx} + \frac{3}{2}|U_2|^2 U_2 - U_2^* + \lambda U_1 = 0. \quad (55)$$

Stationary equations (54) and (55) can be derived from their own Lagrangian, with density

$$\begin{aligned} \mathcal{L} = & \omega(U_1 U_1^* + U_2 U_2^*) + \frac{i}{2} \left(\frac{dU_1}{dx} U_1^* - \frac{dU_1^*}{dx} U_1 + \frac{dU_2}{dx} U_2^* - \frac{dU_2^*}{dx} U_2 \right) \\ & + \frac{3}{4}(|U_1|^4 + |U_2|^4) - \frac{1}{2}(U_1^2 + U_1^{*2} + U_2^2 + U_2^{*2}) + \lambda(U_1 U_2^* + U_1^* U_2). \end{aligned} \quad (56)$$

Then, the following ansatz may be adopted for the *complex* soliton solution sought for:

$$U_{1,2} = A_{1,2} \operatorname{sech}(\mu x) + iB_{1,2} \sinh(\mu x) \operatorname{sech}^2(\mu x), \quad (57)$$

with real $A_{1,2}$, $B_{1,2}$, and μ . The integration of Lagrangian density (56) with this ansatz and subsequent application of the variational procedure gives rise to the following system of equations:

$$3\lambda A_{2,1} - 3(1 - \omega)A_{1,2} + 3A_{1,2}^3 + \frac{3}{5}A_{1,2}B_{1,2}^2 - \mu B_{1,2} = 0, \quad (58)$$

$$\lambda B_{2,1} + \frac{3}{2}B_{1,2} - 3.857B_{1,2}^3 + \frac{3}{5}A_{1,2}^2 B_{1,2} - \mu A_{1,2} = 0, \quad (59)$$

$$2\omega(A_1^2 + A_2^2) + \frac{2\omega}{3}(B_1^2 + B_2^2) + (A_1^4 + A_2^4) - 1.2857(B_1^4 + B_2^4) + \frac{2}{5}(A_1^2 B_1^2 + A_2^2 B_2^2) - 2(A_1^2 + A_2^2) + \frac{2}{3}(B_1^2 + B_2^2) + 4\lambda A_1 A_2 + \frac{4\lambda}{3} B_1 B_2 = 0, \quad (60)$$

where numerical coefficients 3.857 and 1.2857 are defined by some integrals.

A general result, following from both a numerical solution of variational equations (58) - (60) and direct numerical solution of Eqs. (54) and (55), is that a symmetric mode, with $A_1^2 = A_2^2$ and $B_1^2 = B_2^2$, exists at all values of ω in the bandgap (52), and it is the single soliton solution if the coupling constant λ is close enough to 1, i.e., the bandgap (52) is narrow. However, below a critical value of λ (which depends on given ω), the symmetric solution undergoes a bifurcation, giving rise to three branches, one remaining symmetric, while two new ones, which are mirror images to each other, represent nontrivial *asymmetric* solutions.

The bifurcation can be conveniently displayed in terms of an effective asymmetry parameter,

$$\Theta \equiv (U_{1m}^2 - U_{2m}^2) / (U_{1m}^2 + U_{2m}^2), \quad (61)$$

where U_{1m}^2 and U_{2m}^2 are peak powers (maxima of the squared absolute values) of complex fields $U_{1,2}$ in the two cores (note its difference from the asymmetry parameter (28), which was defined in terms of integral energies, rather than peak powers). A complete plot of the SBB for the GSs in the present system, i.e., Θ vs. ω and λ , is displayed in Fig. 8. At $\lambda = 0$, when Eqs. (54) and (55) decouple, the numerical solution matches the exact solution (46) in one core, while the other core is empty. Note the difference of this *supercritical* (alias *forward*) SBB from its weakly *subcritical* (*backward*) counterpart for the solitons in the nonlinear coupler without the BG, which is shown above in Fig. 2.

The bifurcation diagram in Fig. 8 was drawn using numerical results obtained from the solution of Eqs. (54) and (55), but its variational counterpart is very close to it, a relative discrepancy between the VA-predicted and numerically exact values of λ , at which the SBB takes place for fixed ω , being $\lesssim 5\%$. To directly illustrate the accuracy of the VA in the present case, comparison between typical shapes of a stable asymmetric soliton, as obtained from the full numerical solution, and as predicted by the VA, is presented in Fig. 9.

Direct numerical test of the stability of the symmetric and asymmetric solitons in the present model has yielded results exactly corroborating what may be expected: all the asymmetric solitons are stable whenever they exist, while all the symmetric solitons, whenever

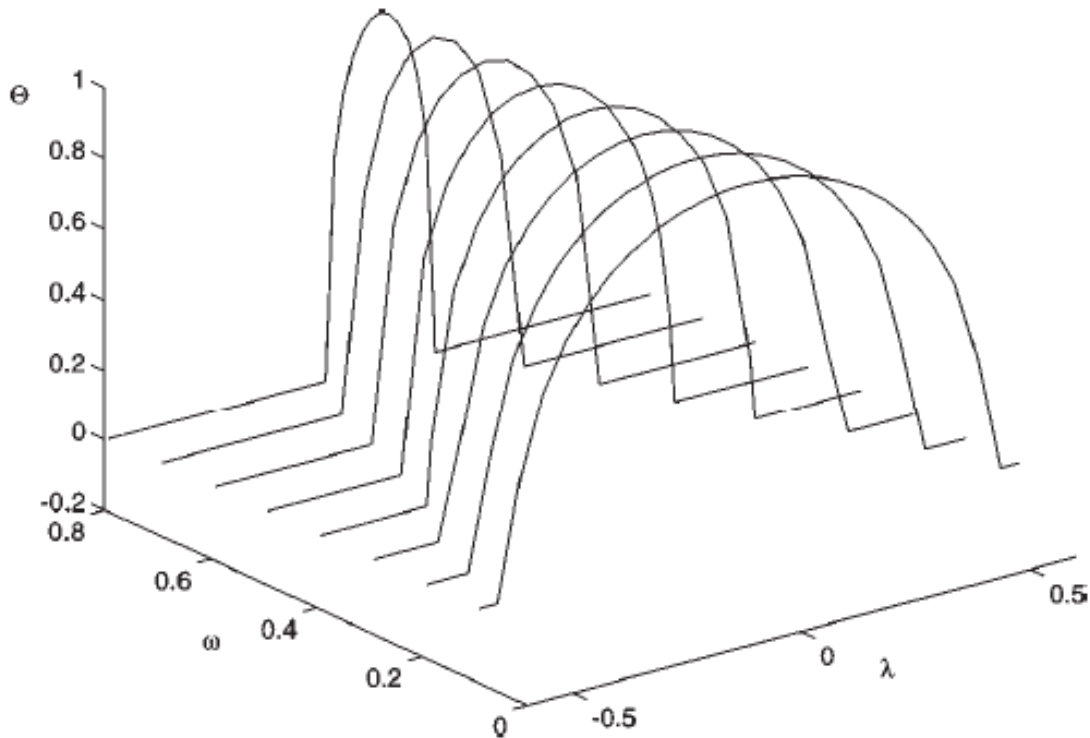


FIG. 8: The symmetry-breaking bifurcation diagram for zero-velocity gap solitons in the model of the dual-core nonlinear optical fiber with identical Bragg gratings written on both cores (as per Ref. [25]).

they coexist with the asymmetric ones, are unstable. However, all the symmetric solitons are stable prior to the bifurcation, where their asymmetric counterparts do not exist.

Lastly, it is relevant to mention that influence of a possible phase shift between the BGs, written in the parallel-coupled cores, on four-component GSs in this system was studied too [26, 27]. In that case, the spontaneous (intrinsic) symmetry breaking is combined with the external symmetry breaking imposed by the mismatch between the BGs.

F. *Bifurcation loops for solitons in couplers with the cubic-quintic (CQ) nonlinearity*

To conclude this section, it is relevant to briefly consider results obtained for the coupler with the CQ nonlinearity, i.e., a combination of competing self-focusing cubic and defocusing

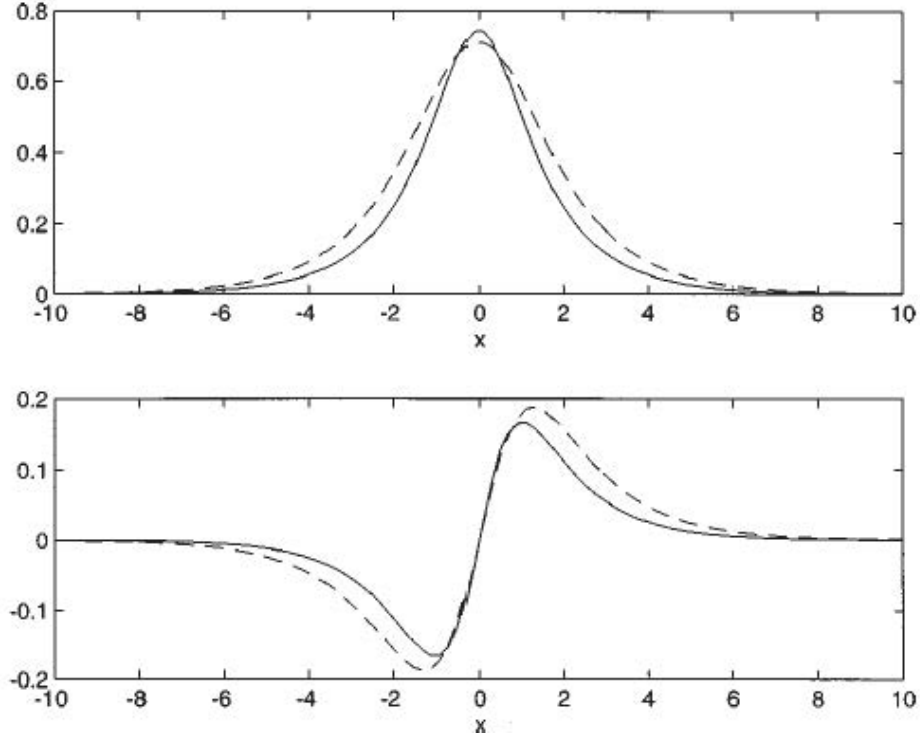


FIG. 9: Shapes of the larger component of the quiescent soliton, U_1 , in the dual-core Bragg grating (as per Ref. [25]). The upper and lower plots show the real and imaginary parts of U_1 . Here, $\omega = 0.5$ and $\lambda = 0.2$.

quintic terms in the respective system of coupled NLSEs:

$$iu_z + u_{\tau\tau} + 2|u|^2u - |u|^4u + \lambda v = 0, \quad (62)$$

$$iv_z + v_{\tau\tau} + 2|v|^2v - |v|^4v + \lambda u = 0, \quad (63)$$

cf. the usual system of Eqs. (1) and (2) with the cubic self-focusing (in both systems, the anomalous sign of the GVD is assumed). By means of straightforward rescaling, the coefficients in front of the nonlinear and dispersive terms may be fixed, without the loss of generality, as written in Eqs. (62) and (63), while coefficient $\lambda > 0$ of the linear inter-core coupling remains a free irreducible parameter. Note that the \mathcal{PT} -symmetric version of the coupler with the CQ nonlinearity and solitons in it were considered too [131].

The CQ combination of the competing nonlinearities, which is assumed in the present system, occurs in various optical media. The realization which is directly relevant to the fabrication of dual-core fibers is provided by chalcogenide glasses [132, 133].

The starting point of the analysis is a well-known exact soliton solution of the single CQ NLS equation [134, 135], to which Eqs. (73) and (74) reduce in the symmetric case:

$$u = v = e^{ikz} U_{\text{symm}}(\tau),$$

$$U_{\text{symm}}(\tau) = \sqrt{\frac{2(k-\lambda)}{1 + \sqrt{1 - 4(k-\lambda)/3} \cosh(2\sqrt{k-\lambda}\tau)}}, \quad (64)$$

where the propagation constant k takes values in the interval of $\lambda < k < \frac{3}{4} + \lambda$. In the limit cases of $k = \lambda$ and

$$k = \frac{3}{4} + \lambda \quad (65)$$

this solution goes over, respectively, into the trivial zero solution, and into the delocalized (continuous-wave, CW) state with a constant amplitude, $u = v = \sqrt{\frac{3}{2}} \exp(i(\frac{3}{4} + \lambda)z)$. The energy of soliton (64), which is defined by the same expression (7) as above, is

$$E_{\text{symm}} = \frac{\sqrt{3}}{2} \ln \left(\frac{\sqrt{3} + 2\sqrt{k-\lambda}}{\sqrt{3} - 2\sqrt{k-\lambda}} \right). \quad (66)$$

Naturally, it diverges in the limit corresponding to Eq. (65).

Following the pattern of the above analysis, asymmetric stationary solitons solutions to Eqs. (62) and (63) are looked for as

$$\{u(z, \tau), v(z, \tau)\} = e^{ikz} \{U(\tau), V(\tau)\}. \quad (67)$$

It can be proved [31] that only solutions with real functions $U(\tau)$ and $V(\tau)$ can be generated by the SBB from the symmetric soliton (64), hence the substitution of expressions (67) with real U and V in Eqs. (73) and (74) leads to a system

$$\frac{d^2 U}{d\tau^2} - kU + \lambda V + 2U^3 - U^5 = 0, \quad (68)$$

$$\frac{d^2 V}{d\tau^2} - kV + \lambda U + 2V^3 - V^5 = 0, \quad (69)$$

which was solved numerically, and the stability of the so found solitons was then identified by dint of direct simulations [31].

The numerical solution of Eqs. (68) and (69) produces a sequence of bifurcation diagrams displayed in Figs. 10 and 11. In these diagrams, the soliton's asymmetry parameter,

$$\epsilon \equiv \frac{U_{\text{max}}^2 - V_{\text{max}}^2}{U_{\text{max}}^2 + V_{\text{max}}^2}, \quad (70)$$

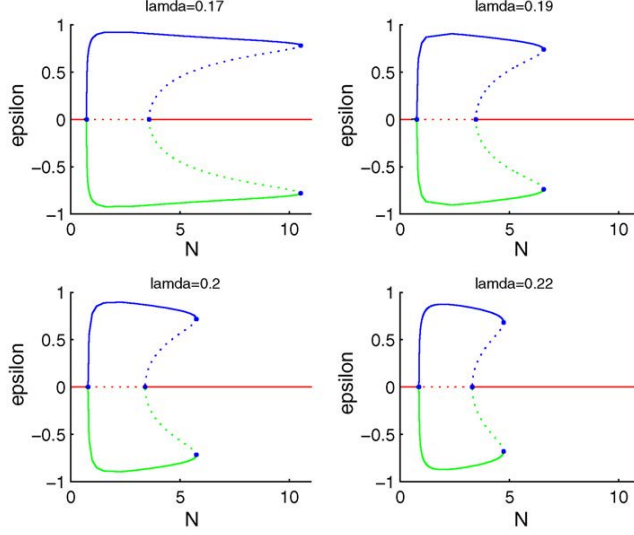


FIG. 10: A set of bifurcation diagrams for symmetric and asymmetric solitons in the plane of the total energy, defined as in Eq. (7), but denoted N here (instead of E), and the asymmetry parameter (70). The diagrams are produced by numerical solution of Eqs. (12) and (13) with the cubic-quintic nonlinearity, at different values of the linear-coupling constant, λ . Stable and unstable branches of the solutions are shown by solid and dashed curves, respectively, and bold dots indicate bifurcation points (as per Ref. [31]).

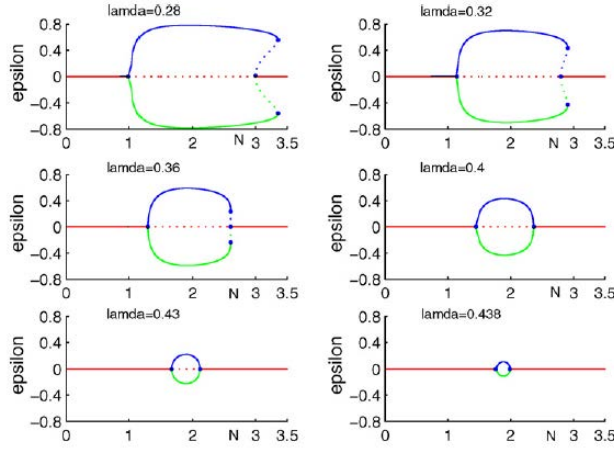


FIG. 11: Continuation of Fig. 10 to larger values of the coupling constant, λ .

where U_{\max}^2 and V_{\max}^2 are the peak powers of the two components of the soliton, is shown versus its total energy. Note the similarity of this definition of the asymmetry to that adopted above in the form of Eq. (61) for solitons in the dual-core BG.

A remarkable peculiarity of the present system is the existence of the *bifurcation loop*:

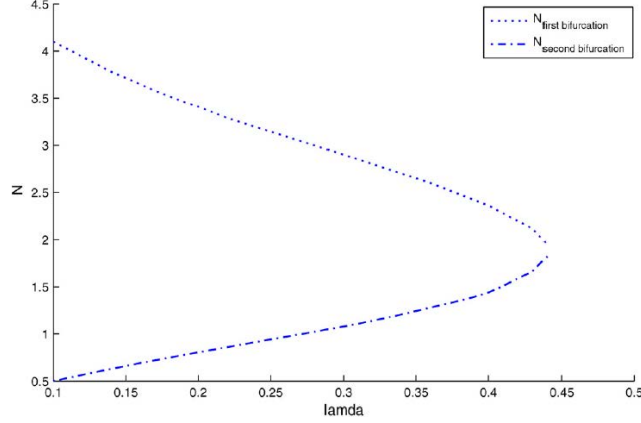


FIG. 12: Values of the energy of the symmetric soliton at which the direct and reverse bifurcations occur in Figs. 10 and 11. The two curves merge and terminate at $\lambda = \lambda_{\max} \approx 0.44$.

as Figs. 10 and 11 demonstrate, the *direct* SBB, which occurs with the increase of the energy, being driven, as above, by the cubic self-focusing, is followed, at larger energies, by the *reverse bifurcation*, which takes place when the dominant nonlinearity becomes self-defocusing, represented by the quintic terms in (68) and (69). The loop exists at $0 < \lambda \leq \lambda_{\max} \approx 0.44$. The direct bifurcation is seen to be always supercritical, while the reverse one, which closes the loop, is subcritical (giving rise to the bistability and concave shape of the loop, on its right-hand side) up to $\lambda \approx 0.40$. In the interval of $0.40 < \lambda < 0.44$, the reverse bifurcation is supercritical, and the (small) loop has a convex form. The picture of the bifurcations is additionally illustrated by Fig. 12, which displays the energy of the symmetric soliton at points of the direct and reverse bifurcations.

Stability and instability of different branches of the soliton solutions can be anticipated on the basis of general principles of the bifurcation theory [93]: the symmetric solution becomes unstable after the direct supercritical bifurcation, and asymmetric solutions emerge as stable ones at this point; eventually, the reverse bifurcation restores the stability of the symmetric solution. In the case when the reverse bifurcation is subcritical and, accordingly, the bifurcation loop is concave on its right side, two branches of asymmetric solutions meet at the turning points, the branches which originate from the reverse-bifurcation point being unstable. These expectations are fully borne out by direct numerical simulations [31]. In particular, in the case when the bifurcation loop has the concave shape, an unstable asymmetric soliton has a choice to evolve into either a still more asymmetric one, or the symmetric soliton (also stable). Numerical results clearly demonstrate that unstable asymmetric solitons

choose the former option, evolving into the *more asymmetric* counterparts.

III. DISSIPATIVE SOLITONS IN DUAL-CORE FIBER LASERS

A. Introduction

Experimental and theoretical studies of fiber lasers are, arguably, the fastest developing area of the modern laser science [136]. A commonly adopted model for the evolution of optical pulses in fiber lasers is based on complex Ginzburg-Landau equations (CGLEs), which readily predict formation of dissipative solitons, alias solitary pulses (SPs), in the lasers [137], due to the stable self-sustained balance of loss and gain, the latter provided by the lasing mechanism (typically, stimulated emission of photons by externally pumped ions of rear-earth metals which are embedded as dopants into the fiber's silica [136]). Important applications of the CGLEs are known in many other fields, including hydrodynamics, plasmas, reaction-diffusion systems, etc., as well as other areas of nonlinear optics [138, 139].

The CGLE of the simplest type is one with the linear dispersive gain and cubic loss (which represents two-photon absorption), combined with the GVD and Kerr nonlinearity. This equation readily produces an exact analytical solution for SPs, in the form of the chirped hyperbolic secant [140, 141], but they are unstable, for an obvious reason: the linear gain destabilizes the zero background around the SP. The most straightforward modification which makes the existence of stable SPs possible is the introduction of the cubic-quintic (CQ) nonlinearity, which includes linear loss (hence the zero background is stable), cubic gain (provided by a combination of the usual linear gain and saturable absorption), and additional quintic loss that provides for the overall stabilization of the model. The CGLE with the CQ nonlinearity was first proposed (in a 2D form) by Sergeev and Petviashvili [142]. A stable SP solution in the 1D version of this equation, which is relevant to modeling fiber lasers, was first reported, in an approximate analytical form, in [82]. These solutions were found by treating the dissipation and gain terms in the CGLE as small perturbations added to the usual cubic NLSE with the anomalous sign of the GVD. Accordingly, the SP was obtained as a perturbation of the standard NLSE soliton. In later works, SPs and their stability in the CQ CGLE were investigated in a broad region of parameters [143]-[147].

Another possibility to produce stable SPs, which is directly relevant to the general topic

of the present article, is to linearly couple the usual cubic CGLE to an additional equation which is dominated by the linear loss. A coupled system of this type was first introduced in Ref. [148], as a model of a dual-core nonlinear dispersive optical fiber, with linear gain, γ_0 , in one (*active*) core, and linear loss, Γ_0 , in the other (*passive*) one:

$$iu_z + \frac{1}{2}u_{\tau\tau} + |u|^2u - i\gamma_0u - i\gamma_1u_{\tau\tau} + \kappa v = 0, \quad (71)$$

$$iv_z + (1/2)v_{\tau\tau} + |v|^2v + i\Gamma_0v + \kappa u = 0. \quad (72)$$

Here, u and v are, respectively, envelopes of the electromagnetic waves in the active and passive cores, z and τ are, as above, the propagation distance and reduced time, cf. Eqs. (1) and (2), κ is the constant of the inter-core coupling, and γ_1 accounts for dispersive loss in the active core (in other words, γ_1 determines the *bandwidth-limited* character of the linear gain). The model assumes the usual self-focusing Kerr nonlinearity and anomalous GVD in the fiber, with the respective coefficients scaled to be 1. The gain in the dual-core fiber can be experimentally realized, similar to the usual fiber lasers, by means of externally pumped resonant dopants [149]. Actually, the dual-core fiber may be fabricated as a symmetric one, with both cores doped, while only one core is pumped by an external light source, which gives rise to the gain in that core.

A more general system of linearly-coupled CGLEs applies to a system of parallel-coupled plasmonic waveguides [150]. The system was further extended for coupled 2D CGLEs, representing stabilized laser cavities [151–153].

It was first theoretically predicted in Refs. [154] and [155] that, adding the parallel-coupled passive core (with loose ends) to the soliton-generating fiber laser, one can improve the stability of the output: while the soliton, being a self-trapped nonlinear mode, remains essentially confined to the active core, small-amplitude noise easily couples to the passive one, where it is radiated away through the loose ends. Independently, a similar dual-core system, with loss in the additional core but without gain in the main one, was proposed as an optical filter cleaning solitons from noise [157]. The basic idea is that, due to the action of the self-focusing nonlinearity, the soliton keeps itself in the core in which it is propagating, while the linear noise tunnels into the parallel core, where it is suppressed by the loss. It was found that the best efficiency of the filtering is attained not with very strong loss (Γ_0) in the extra core, but rather at $\Gamma_0 \sim \kappa$, see Eq. (72) [157]. Another possible application of the dual-core system with the gain in the *straight core* (the one into which the input signal

is coupled) and losses in the *cross core* (the one linearly coupled to the straight core) was proposed for the design of a nonlinear amplifier of optical signals: a very weak (linear) input would pass into the cross core, and would be lost there, while the input whose power exceeds a certain threshold, making it a sufficiently nonlinear mode, stays in the straight core, being amplified there [14].

In Ref. [148], the possibility of the existence of stable SPs in the system of Eqs. (71) and (72) was predicted in the framework of an analytical approximation, that treated both the coupling and gain/loss terms as small perturbations. The stability of the so predicted pulses was then verified by direct simulations [158]. Further, it was demonstrated that the system may be simplified, by dropping the nonlinear and GVD terms in Eq. (72), where they are insignificant (the nonlinearity may be omitted as the amplitude of the component in the passive core is small, and the GVD is negligible, as the linear properties of the passive core are dominated by the loss term). On the other hand, an extra linear term, namely, a phase-velocity mismatch between the cores, should be added to Eq. (72), as the respective effect may be essential (see below). As a result, a pair of SP solutions for the simplified system was found in an *exact analytical form* (which is displayed below), the pulse with a larger amplitude being stable in a vast parameter region, while its counterpart with the smaller amplitude is always unstable [159, 161]. The basic results are presented, in some detail, in subsections following below. A detailed review of these and related results can be found in Ref. [67].

B. The exact SP (solitary-pulse) solution

The most fundamental coupled system, which has the cubic nonlinearity in the active core only, is based on the following system, which is simplified in comparison with original equations (71) and (72) [159]:

$$iu_z + \left(\frac{1}{2} - i\gamma_1\right) u_{\tau\tau} + (\sigma + i\gamma_2) |u|^2 u - i\gamma_0 u + v = 0, \quad (73)$$

$$iv_z + k_0 v + i\Gamma_0 v + u = 0, \quad (74)$$

where $\kappa = 1$ is fixed by means of scaling, $\sigma = +1$ and -1 correspond to the anomalous and normal GVD in the active core (assuming that the actual nonlinearity is self-focusing, which is the case in optical fibers, this sign parameter may be placed in front of the cubic term,

as written in Eq. (73), although σ originally appears in front of the second derivative), $\gamma_2 \geq 0$ accounts for cubic loss (two-photon absorption), and k_0 is the above-mentioned phase-velocity mismatch between the cores.

The *exact* SP solution to Eqs. (73) and (74) can be found in the analytical form suggested by the well-known solution [140, 141] of the cubic CGLE:

$$\{u, v\} = \{A, B\} e^{ikz} [\operatorname{sech}(\chi\tau)]^{1+i\mu}, \quad (75)$$

where all the constants but B are real. Coefficient μ , which determines the *chirp* of the pulse, is

$$\mu = \frac{\sigma \sqrt{9(1 - 2\sigma\gamma_1\gamma_2)^2 + 8(2\gamma_1 + \sigma\gamma_2)^2} - 3(1 - 2\sigma\gamma_1\gamma_2)}{2(2\gamma_1 + \sigma\gamma_2)}. \quad (76)$$

The complex and real amplitudes, B and A , are given by expressions

$$B = (k - k_0 - i\Gamma_0)^{-1} A, \quad (77)$$

$$A^2 = \sigma \frac{[(1 - 2\sigma\gamma_1\gamma_2)(2 - \mu^2) + 3\mu(2\gamma_1 + \sigma\gamma_2)] \chi^2}{2(1 + 2\gamma_2^2)}, \quad (78)$$

with the two remaining real parameters χ and k determined by one complex equation,

$$k + i\gamma_0 - (k - k_0 - i\Gamma_0)^{-1} = \left(\frac{1}{2} - i\gamma_1\right) (1 + i\mu)^2 \chi^2. \quad (79)$$

In the further analysis of the SP solutions, one may set $\gamma_2 = 0$, as the two-photon absorption is insignificant in silica fibers. Then, χ^2 can be eliminated from Eq. (79),

$$\chi^2 = \frac{8\gamma_0\gamma_1}{8\gamma_1^2 + 3 - \sigma\sqrt{9 + 32\gamma_1^2}} \left(1 - \frac{\Gamma_0}{\gamma_0 [(k - k_0)^2 + \Gamma_0^2]}\right), \quad (80)$$

and one arrives at a final cubic equation for k :

$$k [(k - k_0)^2 + \Gamma_0^2] - (k - k_0) = \frac{\sigma\sqrt{9 + 32\gamma_1^2}}{2\gamma_1} [\gamma_0 (k - k_0)^2 - \Gamma_0 (1 - \gamma_0\Gamma_0)], \quad (81)$$

which may give rise to one or three real solutions. Physical solutions are those which make expression (80) positive. In particular, the number of the physical solutions changes when expression (80) vanishes, which happens at $k_0^2 = (\gamma_0\Gamma_0)^{-1} (1 - \gamma_0\Gamma_0) (\Gamma_0 - \gamma_0)^2$.

The above results may be cast in a more explicit form in the case of no wavenumber mismatch between the cores, $k_0 = 0$. Note that the SP solution is of interest if it is stable, a necessary condition for which is the stability of the zero background, i.e., the trivial solution,

$u = v = 0$. If $k_0 = 0$, necessary conditions for the stability of the zero solution are $\gamma_0 < \Gamma_0$ and $\gamma_0\Gamma_0 < 1$. It is natural to focus on the case when gain γ_0 is close to the maximum value, $(\gamma_0)_{\max} \equiv 1/\Gamma_0$, admitted by the latter condition, i.e.,

$$0 < 1 - \gamma_0\Gamma_0 \ll 1 \quad (82)$$

(then, condition $\gamma_0 < \Gamma_0$ reduces to $\Gamma_0 > 1$). In this case, Eq. (81) may be easily solved. The first root has small k , which yields unphysical solutions, with $\chi^2 < 0$. Two other roots for k are physically relevant ones, in which γ_0 may be replaced by $1/\Gamma_0$, due to relation (82):

$$4k = \frac{\sigma\sqrt{9 + 32\gamma_1^2}}{\Gamma_0\gamma_1} \pm \sqrt{\frac{9 + 32\gamma_1^2}{\Gamma_0^2\gamma_1^2} - 16(\Gamma_0^2 - 1)}, \quad (83)$$

$$\chi^2 = \frac{8\gamma_1 k^2 (k^2 + \Gamma_0^2)^{-1}}{\Gamma_0 \left(3 + 8\gamma_1^2 - \sigma\sqrt{9 + 32\gamma_1^2}\right)}. \quad (84)$$

Expression (84) is always positive, while a nontrivial existence condition for these two solutions follows from Eq. (83): k must be real, which means that

$$9\gamma_1^{-2} + 32 > 16\Gamma_0^2 (\Gamma_0^2 - 1). \quad (85)$$

Thus, Eqs. (83) and (84), along with Eqs. (75), (76), (77), (78), and (80), (81), furnish the SP solutions in the region of the major interest, and Eq. (85) is a fundamental condition which secures the existence of these solutions.

If condition (85) holds, one has the following set of solutions: (i) the stable zero state, (ii) the broader SP with a smaller amplitude, corresponding to smaller k^2 , i.e., with sign \pm in expression (83) chosen opposite to σ , and (iii) the narrower pulse with a larger amplitude, corresponding to larger k^2 , i.e., with \pm in (83) chosen to coincide with σ . Basic principles of the bifurcation theory [93] suggest that stable and unstable solutions alternate, hence, because the trivial solution is stable, the larger-amplitude narrower pulse ought to be stable too, while the intermediate broader pulse with the smaller amplitude is always unstable, playing the role of a *separatrix* between the two *attractors*. This expectation is, generally, corroborated by numerical results [63, 64, 158, 159], as shown in some detail below. Note that the above-mentioned SP waveform [140, 141], which suggested ansatz (75) for the exact solutions under the consideration, is, by itself, *always unstable* as the solution of the single cubic CGL equation.

C. Special cases of stable SPs (solitary pulses)

There are two particular cases of physical interest that should be considered separately. The first corresponds to the model with $\gamma_1 = 0$ (negligible dispersive loss). In this case, the above SP solution may only exist in the system with anomalous GVD, $\sigma = +1$. Special consideration of this case is necessary because the above formulas are singular for $\gamma_1 = 0$. An explicit result for this situation can be obtained *without* adopting condition (82): the solutions take the form of Eq. (75) with $\mu = 0$ (no chirp), Eq. (78) being replaced by $A^2 = \chi^2$, while Eqs. (79) and (78) become

$$\begin{aligned} k - k_0 &= \pm \sqrt{\Gamma_0 \gamma_0^{-1} (1 - \gamma_0 \Gamma_0)}, \\ \chi^2 &= 2k_0 \pm 2(\gamma_0 + \Gamma_0) \sqrt{(\gamma_0 \Gamma_0)^{-1} (1 - \gamma_0 \Gamma_0)}. \end{aligned} \quad (86)$$

Two solutions corresponding to both signs in Eqs. (86) exist simultaneously, i.e., $\chi^2 > 0$ holds for both of them, provided that $k_0^2 > (\gamma_0 \Gamma_0)^{-1} (1 - \gamma_0 \Gamma_0) (\gamma_0 + \Gamma_0)^2$. However, one can check that this inequality contradicts the stability conditions of the zero state, therefore only *one* solution given by Eqs. (86) may exist in the case of interest. General principles of the bifurcation theory [93] suggest that this single nontrivial solution is automatically unstable in the case of $\gamma_1 = 0$, once the trivial one is stable.

The other specially interesting case is that of zero GVD, corresponding to the physically important situation when the carrier wavelength is close to the zero-dispersion point [102] of the optical fiber. In this case, Eq. (74) does not change its form, while Eq. (73) is replaced by

$$iu_z - iu_{\tau\tau} + |u|^2 u - i\gamma_0 u + v = 0 \quad (87)$$

(in the absence of the GVD, both signs of σ are equivalent, hence $\sigma = +1$ is fixed here, and normalization $\gamma_1 \equiv 1$ may be adopted). Explicit solutions can be obtained, as well as in the general case considered above, by assuming $k_0 = 0$ and taking $\gamma_0 \Gamma_0$ close to 1. Then, expressions (78) and (76) are replaced by $\mu = \sqrt{2}$, $A^2 = 3\sqrt{2}\chi^2$, while solutions (83) and (84) take the form of

$$k = \sqrt{2}\Gamma_0^{-1} \pm \sqrt{2\Gamma_0^{-2} - \Gamma_0^2 + 1}, \quad \chi^2 = \Gamma_0^{-1} (\Gamma_0^2 + k^2)^{-1} k^2, \quad (88)$$

and the existence condition (85) becomes very simple, $\Gamma_0^2 < 2$. Thus, in the zero-GVD case both SP solutions (88) exist simultaneously, suggesting that the one with the larger value of k^2 may be *stable*.

Lastly, it may be interesting to consider another particular case, with normal GVD, $\sigma = -1$, and small dispersive-loss coefficient, $\gamma_1 \ll 1$. In this case, there are two nontrivial SP solutions, the one with the larger amplitude, that has the chance to be stable, being

$$\mu = -\frac{3}{2}\gamma_1^{-1}, A^2 = \frac{3}{2}(\gamma_1\Gamma_0)^{-1}, k = -\frac{3}{2}\gamma_1^{-1}, \chi^2 = \frac{4}{3}(\Gamma_0^{-1}\gamma_1). \quad (89)$$

The large value of μ in this solution implies that the pulse is strongly chirped. Obviously, the latter solution disappears in the limit of $\gamma_1 \rightarrow 0$, in accordance with the above-mentioned negative result (no stable SP) for the case of $\gamma_1 = 0$.

D. Stability of the solitary pulses and dynamical effects

As mentioned above, the SP cannot be stable unless its background, $u = v = 0$, is stable. To explore the stability of the zero solution, infinitesimal perturbations are substituted in the linearized version of Eqs. (73) and (74): $\{u, v\} = \{u_1, v_1\} e^{i(qz - \omega t)}$, where ω and q are an arbitrary real frequency and the corresponding propagation constant (generally speaking, a complex one). The stability condition is $\text{Im}(q) = 0$, which must hold at all real ω . This condition leads an inequality that should be valid at all $\omega^2 \geq 0$,

$$\Gamma_0(\gamma_0 - \gamma_1\omega^2) \left[1 + \frac{(2k_0 + \omega^2)^2}{4(\Gamma_0 - \gamma_0 + \gamma_1\omega^2)^2} \right] \leq 1. \quad (90)$$

If the GVD coefficient is zero, i.e., Eq. (73) is replaced by Eq. (87), expression $(2k_0 + \omega^2)^2$ in Eq. (90) is replaced by $4k_0^2$. An obvious corollary of Eq. (90) is

$$\gamma_0 < \Gamma_0, \quad (91)$$

i.e., the trivial solution may be stable only if the loss in the passive core is stronger than the gain in the active one. Further, in the case of zero wavenumber mismatch between the cores, $k_0 = 0$, which was considered above (see Eqs. (83) and (84)), a simple necessary stability condition is obtained from Eq. (90) at $\omega = 0$ (as was already mentioned above, see Eq. (82)): $\gamma_0\Gamma_0 > 1$.

Stability regions of the SP solutions in the parameter space of the system were identified in Refs. [158] and [161] in a numerical form, combining the analysis of the necessary stability condition of the zero background, given by Eq. (90), and direct simulations of Eqs. (73) and (74) for perturbed SPs. As said above, the case of major interest is the one with

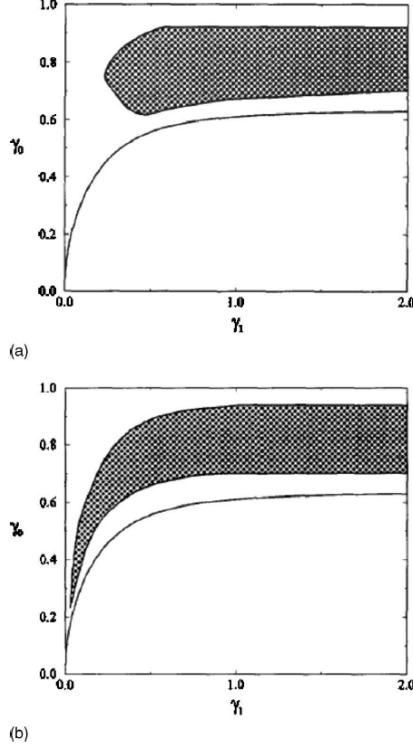


FIG. 13: The stability region (shaded) in the parameter plane of the exact solitary-pulse solution (75) of Eqs. (73) and (74), for the case of $k_0 = \gamma_2 = 0$ and $\gamma_0\Gamma_0 = 0.9$, as per Refs. [159] and [67]. Panels (a) and (b) display results for the anomalous and normal GVD, respectively, i.e., $\sigma = +1$ and $\sigma = -1$ in Eq. (73). The separate curve shows the existence boundary given by Eq. (85).

$k_0 = \gamma_2 = 0$ and $\gamma_0\Gamma_0$ close to 1. For this case, the stability regions are displayed in Fig. 13, and separately in Fig. 14 for the zero-GVD system. In each case, there is a single stable SP (but the system is a *bistable* one, as the stable SP always coexists with the stable zero solution).

Another cross section of the stability region in the full three-dimensional parameter space of the model is represented by region II in Fig. 15, for the normal-GVD case ($\sigma = -1$), with $\gamma_1 = 1/18$ (this value is a typical one corresponding to physically relevant parameters of optical fibers). Note that this plot reveals a very narrow region (area III), in which the zero solution is stable, while the SP is not.

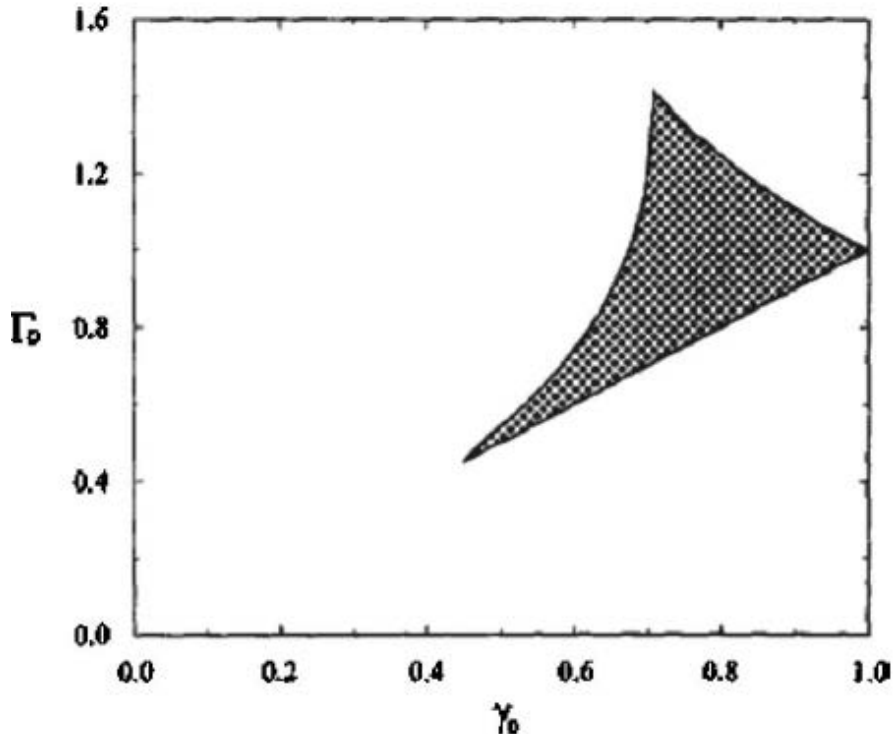


FIG. 14: The same as in Fig. 13, but for the exact solitary-pulse solution (88), in the system with zero dispersion (as per Refs. [159] and [67]).

E. Interactions between solitary pulses

It is well known that the sign of the interaction between ordinary solitons is determined by the phase shift between them, $\Delta\phi$: the interaction is attractive for in-phase soliton pairs, with $\Delta\phi = 0$, and repulsive for $\Delta\phi = \pi$ [160]. However, this rule does not apply to the SPs in the present model with the normal sign of the GVD ($\sigma = -1$ in Eq. (73)), which feature strong chirp in their phase structure (see, e.g., the expression for chirp μ in solution (89), with $\gamma_1 \ll 1$). It was found [161] that, irrespective of the value of $\Delta\phi$, the SPs in the normal-GVD model *attract* each other, and eventually merge into a single pulse, as shown in Fig. 16.

On the other hand, in-phase pairs of the SPs in the anomalous-GVD system, with $\sigma = +1$, readily form robust bound states [162]. Three-pulse bound states were found too, but they are unstable against symmetry-breaking perturbations, which split them according to the scheme $3 \rightarrow 2 + 1$.

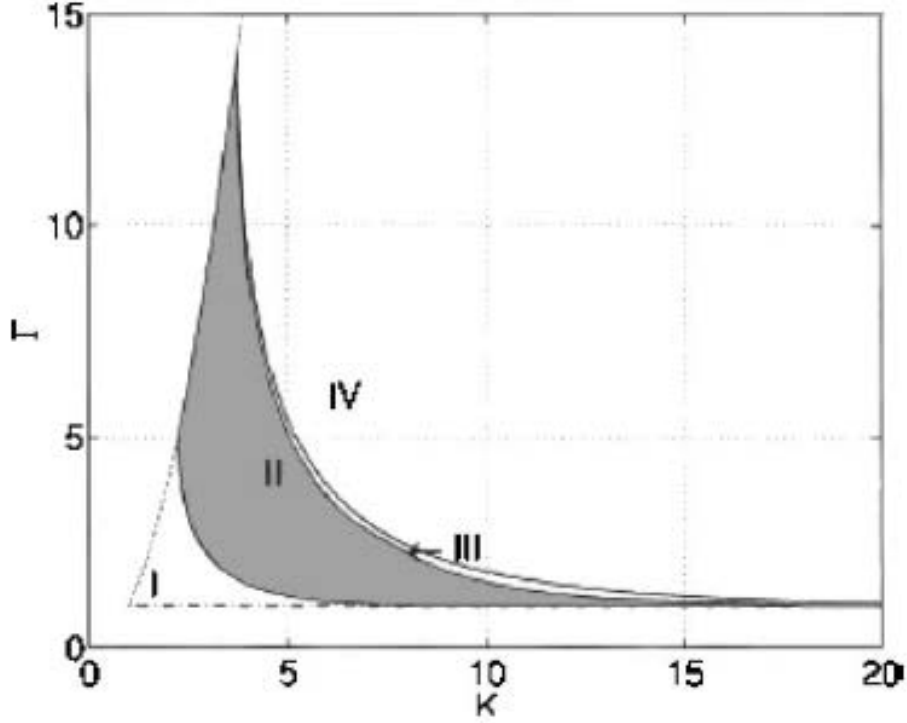
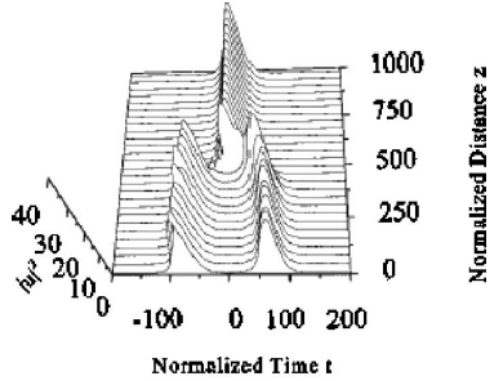


FIG. 15: Stability regions of the zero solution, and existence and stability regions for the exact solitary-pulse solution (75) of Eqs. (73) and (74), as per Refs. [159] and [67], in the plane of parameters $K \equiv 1/\gamma_0$ and $\Gamma \equiv \Gamma_0/\gamma_0$, in the model with the normal GVD ($\sigma = -1$), $k_0 = \gamma_2 = 0$, and $\gamma_1 = 1/18$. Region I: the zero background is unstable. Region II: the solitary pulse is stable. Region III: the zero background is stable, while the solitary pulse is not, decaying to zero in direct simulations. Region IV: the solitary-pulse solution does not exist. In the region located outside of region I, which is bordered by curves $\gamma_0\Gamma_0 = 1$ (the dotted curve) and $\Gamma_0 = \gamma_0$ (the dotted-dashed curve), the zero solution is certainly unstable, as condition (82) does not hold in that region. In region I, zero background is unstable even though condition (82) holds in this region.

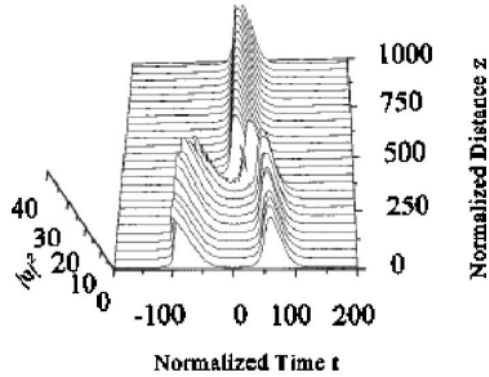
F. CW (continuous-wave) states and dark solitons (“holes”)

In addition to the SPs, Eqs. (73) and (74) also admit CW states with constant amplitudes,

$$u = a \exp(ikz - i\omega\tau), \quad v = b \exp(ikz - i\omega\tau). \quad (92)$$



(a)



(b)

FIG. 16: Merger of chirped solitary pulses in the system of Eqs. (73) and (74) with normal GVD ($\sigma = -1$). Other parameters are $k_0 = \gamma_2 = 0$, $\gamma_0 = 0.2$, $\Gamma_0 = 0.8$, and $\gamma_1 = 1/18$. The initial phase shift between the pulses is $\Delta\phi = 0$ (a) and $\Delta\phi = \pi$ (b). The results are displayed as per Refs. [162] and [67].

The propagation constant and amplitudes of this solution can be easily found in the case of $\gamma_2 = 0$:

$$\begin{aligned}
 b &= (k - k_0 - i\Gamma_0)^{-1} a, \\
 k - k_0 &= \pm \sqrt{\Gamma_0 \tilde{\gamma}_0^{-1} (1 - \Gamma_0 \tilde{\gamma}_0)}, \\
 \sigma a^2 &= k_0 \pm \sqrt{(\Gamma_0 \tilde{\gamma}_0)^{-1} (1 - \Gamma_0 \tilde{\gamma}_0) (\Gamma_0 - \tilde{\gamma}_0)}, \tag{93}
 \end{aligned}$$

where $\tilde{\gamma}_0 \equiv \gamma_0 - \gamma_1 \omega^2$. According to this, at given ω there may exist two CW states with different amplitudes, provided that $k_0^2 \geq (\Gamma_0 \tilde{\gamma}_0)^{-1} (1 - \Gamma_0 \tilde{\gamma}_0) (\Gamma_0 - \tilde{\gamma}_0)^2$, and a single one in the opposite case. The CWs may be subject to the MI (modulational instability), which was investigated in detail [97, 164]. In particular, all CWs are unstable at $k_0 = 0$, although

the character of the MI is different for the normal and anomalous signs of the GVD [164]. Direct simulations demonstrate that the development of the MI splits the CW state into an array of SPs.

At $k_0 \neq 0$, there is a parameter region in the normal-GVD regime (with $\sigma = -1$) where the CW solutions are stable, which suggests to explore solutions in the form of dark solitons (which are frequently called “holes”, in the context of the CGLEs [165]). Such solutions of Eqs. (73) and (74) can be found in an exact analytical form based on the following ansatz [163] (cf. the form of exact solution (75) for the bright SP):

$$u = \frac{(2 - e^{2\chi\tau}) A}{(1 + e^{2\chi\tau})^{1-i\mu}} e^{ikz - i\mu\chi\tau}, v = \frac{u}{k_0 - k + i\Gamma_0}, \quad (94)$$

with $\mu = (3/4\gamma_1) + \sqrt{(9/4\gamma_1)^2 + 2}$ (in the case of $\gamma_2 = 0$), the other parameters, A , χ , and k , being determined by cumbersome algebraic equations. Numerical analysis demonstrates that dark solitons (94) are stable in a small parameter region, as shown in Fig. 17.

G. Evolution of solitary pulses beyond the onset of instability

Direct simulations of the system with normal GVD, $\sigma = -1$ in Eq. (74), demonstrate that unstable SPs (in the case when stable solutions do not exist) either decay to zero (if the zero background is stable), or blow up, initiating a transition to a “turbulent” state, if the background is unstable. A different behavior of unstable SPs was found in Ref. [167] in the model with the anomalous GVD ($\sigma = +1$). If the instability of the zero background is weak, it does not necessarily lead to the blow-up. Instead, it may generate a small-amplitude background field featuring regular oscillations. In that case, the SP sitting on top of such a small-amplitude background remains completely stable, as shown in Fig. 18. The proximity of this state to the stability border is characterized by the *overcriticality parameter*,

$$\epsilon \equiv (\gamma_0 - (\gamma_0)_{\text{cr}}) / (\gamma_0)_{\text{cr}}, \quad (95)$$

where $(\gamma_0)_{\text{cr}}$ is the critical size of the linear gain at which the instability of the zero solution sets in, at given values of γ_1 , k_0 , and Γ_0 . An example of the stable pulse found on top of the finite background, which is displayed in Fig. 18, pertains to $\epsilon = 0.025$.

At larger but still moderate values of the overcriticality, such as $\epsilon = 0.157$ in Fig. 19, the background oscillations become chaotic, while keeping a relatively small amplitude. As

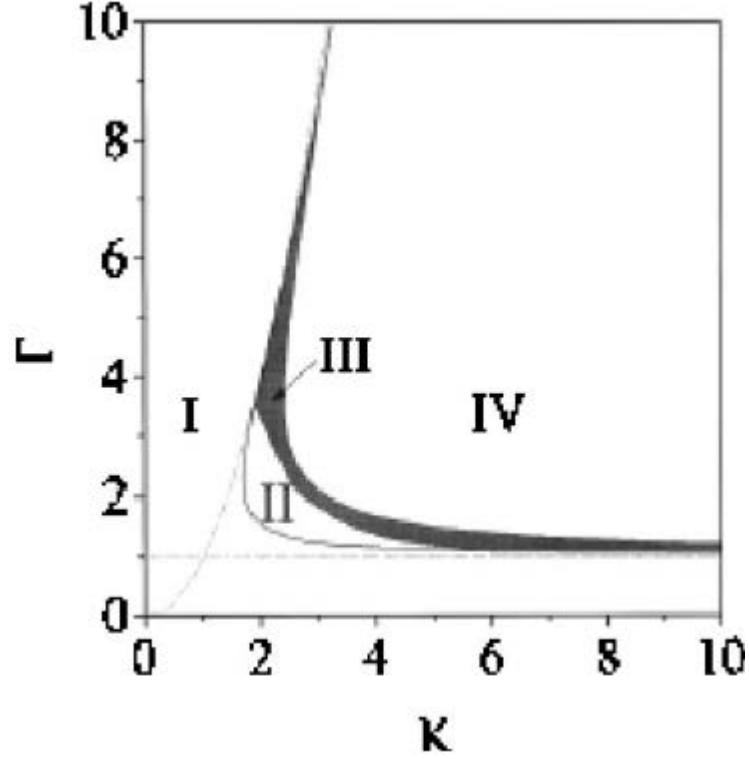


FIG. 17: Regions of the existence and stability of the CW state and dark soliton (94), produced by Eqs. (73) and (74) in the same parameter plane as in Fig. 15, in the case of $\sigma = -1$, $\gamma_2 = 0$, $\gamma_1 = 1/7$, and $k_0 = 2\gamma_2$. The existence region of the CW solution is confined by the dashed lines, $\Gamma_0 = 1$ and $\gamma_0\Gamma_0 = 1$. In regions I and IV, the CW is unstable. In region II, it is stable, while the dark soliton is not. In region III, both the CW and dark-soliton solutions are stable. The results are displayed as per Refs. [161] and [67].

a result of the interaction with this chaotic background, the SP remains stable as a whole, featuring a random walk. The walk shows a typically diffusive behavior, with the average squared shift in the τ -direction growing linearly with z [167]. The randomly walking pulses may easily form bound states, which then feature synchronized random motion. Finally, at essentially larger values of the overcriticality, $\epsilon \gtrsim 1$, the system goes over into a turbulent state, which may be interpreted as a chaotic gas of solitary pulses [167].

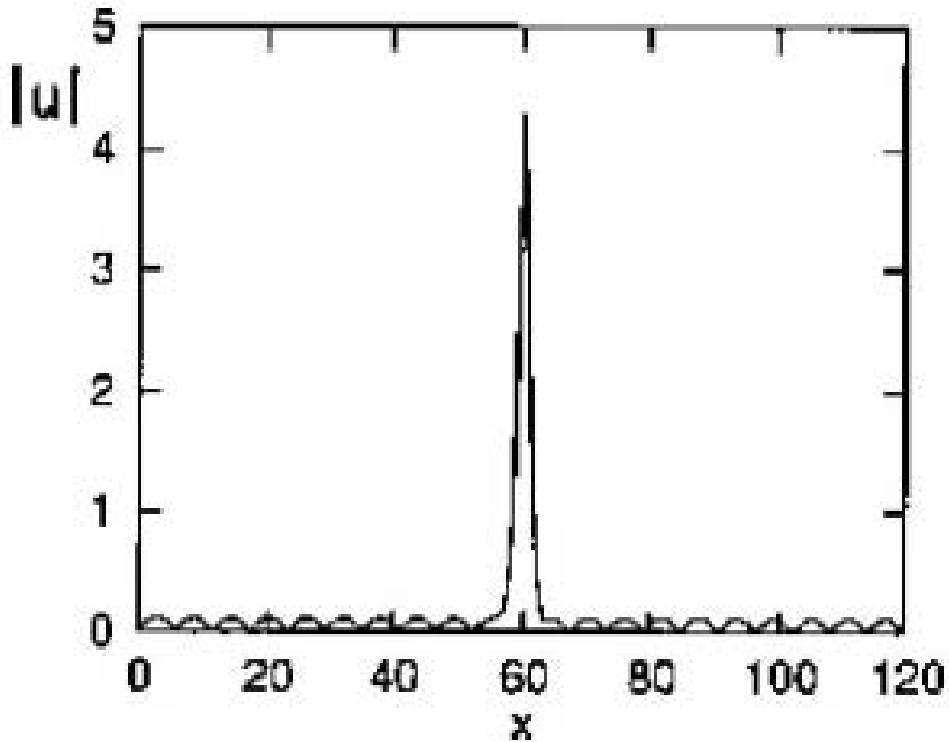


FIG. 18: An example of a stable solitary pulse in the system of Eqs. (73) and (74), with the anomalous GVD ($\sigma = +1$), which exists on top of the small-amplitude background featuring regular oscillations, in the case when the zero background is weakly unstable (the respective overcriticality is $\epsilon = 0.025$, see Eq. (95)). Parameters are $k_0 = 0$, $\gamma_0 = 0.54$, $\Gamma_0 = 1.35$, $\gamma_1 = 0.18$. The results are displayed as per Refs. [167] and [67].

IV. SOLITON STABILITY IN \mathcal{PT} (PARITY-TIME)-SYMMETRIC NONLINEAR DUAL-CORE FIBERS

The dual-core fibers with equal (mutually balanced) gain and loss in the cores offer a natural setting for the realization of the \mathcal{PT} symmetry, in addition to other optical media, where this symmetry was proposed theoretically [71], [72], [74]-[77], [79]-[81], [131], and implemented experimentally [168, 169].

The basic model of the \mathcal{PT} -symmetric nonlinear coupler is based on the equations similar to Eqs. (1) and (2), in which $\gamma > 0$ is the gain-loss coefficient, and the coefficient of the

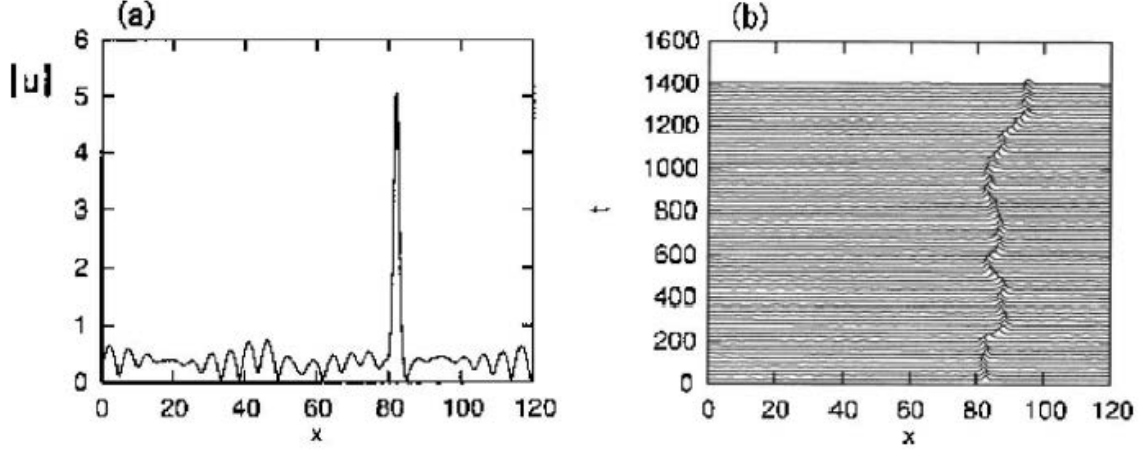


FIG. 19: (a) An example of a solitary pulse which remains stable, as a whole, on top of the background featuring chaotic oscillations, at overcriticality $\epsilon = 0.157$. Parameters are the same as in Fig. 18, except for $\gamma_0 = 0.61$. (b) The random walk of the stable pulse from (a), driven by its interaction with the chaotic background. The results are displayed as per Refs. [167] and [67].

inter-core coupling (K in Eqs. (1) and (2)) is scaled to be 1 [68, 69]:

$$iu_z + (1/2)u_{tt} + |u|^2u - i\gamma u + v = 0, \quad (96)$$

$$iv_z + (1/2)v_{tt} + |v|^2v + i\gamma v + u = 0. \quad (97)$$

Note that the \mathcal{PT} -balanced gain and loss in this system correspond to the border between stable and unstable settings: if the loss coefficient in Eq. (97) is replaced by an independent one, $\Gamma > 0$ (different from the gain factor γ in Eq. (97)), the zero solution, $u = v = 0$, is unstable at $\gamma > \Gamma$, and may be stable at $\gamma < \Gamma$, see Eq. (91) above.

Obviously, *any* solution to the NLSE (with a frequency shift), $iU_z + (1/2)U_{tt} + |U|^2U \pm \sqrt{1 - \gamma^2}U = 0$, gives rise to two *exact* solutions of the \mathcal{PT} -symmetric system, provided that condition $\gamma \leq 1$ holds:

$$v = \left(i\gamma \pm \sqrt{1 - \gamma^2} \right) u = U(z, t). \quad (98)$$

For $\gamma = 0$, solutions (98) with $+$ and $-$ amount, respectively, to symmetric and antisymmetric modes in the dual-core coupler, therefore the respective solutions (98) may be called \mathcal{PT} -symmetric and \mathcal{PT} -antisymmetric ones. In the limit of $\gamma = 1$, two solutions (98) reduce to a single one, $v = iu = U(z, t)$. In particular, \mathcal{PT} -symmetric and antisymmetric solitons,

with arbitrary amplitude η , are generated by the NLSE solitons,

$$U(z, t) = \eta \exp\left(i\left(\eta^2/2 \pm \sqrt{1-\gamma^2}\right)z\right) \operatorname{sech}(\eta t). \quad (99)$$

As concerns stability of the solitons in this system, it is relevant to compare it to the stability in the usual coupler model, with $\gamma = 0$. As explained above (see Eq. (17)), the symmetric solitons in the nonlinear coupler are unstable against the spontaneous symmetry breaking at

$$\eta^2 > \eta_{\max}^2(\gamma = 0) \equiv 4/3 \quad (100)$$

[34], while antisymmetric solitons are always unstable [39] (although their instability may be weak).

The analysis of the instability of the usual two-component symmetric solitons against antisymmetric perturbations, $\delta u = -\delta v$, which leads to the exact result (100), see Eqs. (14) and (16) above, can be extended for the \mathcal{PT} -symmetric system. The respective perturbation δu at the critical point, $\eta^2 = \eta_{\max}^2$, obeys the linearized equation,

$$\left\{4\sqrt{1-\gamma^2} - d^2/dt^2 + \eta_{\max}^2 [1 - 6\operatorname{sech}^2(\eta_{\max}t)]\right\} \delta u = 0, \quad (101)$$

which is the respective generalization of Eq. (16). This equation with the Pöschl-Teller potential is solvable, yielding

$$\eta_{\max}^2(\gamma) = (4/3)\sqrt{1-\gamma^2}. \quad (102)$$

This analytical prediction was verified by direct simulations of the perturbed evolution of the \mathcal{PT} -symmetric solitons. The simulations were run by adding finite initial antisymmetric perturbations, at the amplitude level of $\pm 3\%$, to the symmetric solitons. For \mathcal{PT} -antisymmetric solitons, the instability boundary was identified solely in the numerical form, by running the simulations with initial symmetric perturbations. The results are summarized in Fig. 20, as per Ref. [68]. The numerically identified stability border for the symmetric solitons goes somewhat below the analytical one (102) because the finite perturbations used in the simulations are actually not quite small. Taking smaller perturbations, one can obtain the numerical stability border approaching the analytical limit. For instance, at $\gamma = 0.5$, the perturbations with relative amplitudes $\pm 5\%$, $\pm 3\%$, and $\pm 1\%$ give rise to the stability border at $\eta_{\max}^2 = 1.02$, 1.055, and 1.08, respectively, while Eq. (102) yields $\eta_{\max}^2 \approx 1.15$ in the same case. As concerns the \mathcal{PT} -antisymmetric solitons, a detailed analysis demonstrated that

they are completely unstable [69], while the numerically found boundary delineates an area in which the instability is very weak.

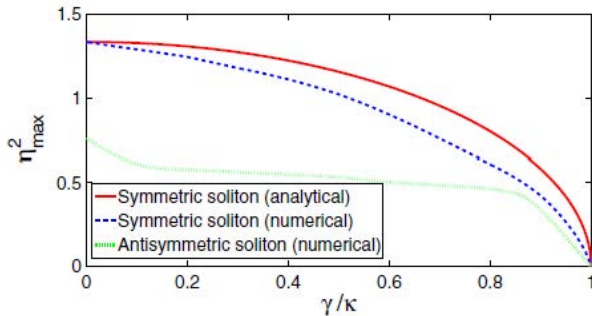


FIG. 20: The analytically predicted stability border (102) for the \mathcal{PT} -symmetric solitons, and its counterpart produced by systematic simulations of the perturbed evolution of the solitons, as per Ref. [68]. An effective numerical stability border for the \mathcal{PT} -antisymmetric solitons is shown too, although all the antisymmetric solitons are, strictly speaking, unstable [69] (the numerically identified stability area for them implies very weak instability). The solitons with amplitude η are stable at $\eta < \eta_{\max}$. In this figure, γ/κ is identical to γ , as the inter-core coupling coefficient is fixed by scaling to be $\kappa = 1$, see the text.

It is relevant to stress that, being the stability boundary of the \mathcal{PT} -symmetric solitons, the present system, unlike the usual dual-core coupler (see above), cannot support asymmetric solitons, as the balance between the gain and loss is obviously impossible for them. Accordingly, the instability of solitons with $\eta > \eta_{\max}$ leads to a blowup of the pumped field, u , and decay of the attenuated one, v , in direct simulations (not shown here).

The presence of the gain and loss terms in Eqs. (96) and (97) does not break their Galilean invariance, which suggests to consider collisions between moving stable solitons, setting them in motion by means of *boosting*, i.e., replacing

$$\{u, v\} \rightarrow \{u, v\} \exp(\pm i\chi t) \quad (103)$$

in the initial state ($z = 0$), with arbitrary frequency shift χ . Simulations demonstrate that the collisions are always elastic, see a typical example in Fig. 21.

The limit case of $\gamma = 1$ may be considered as one of “supersymmetry”, because the inter-core coupling constant and gain-loss coefficients are equal in Eqs. (96) and (97) in this case. According to Eq. (102), the stability region of the solitons in the supersymmetric systems

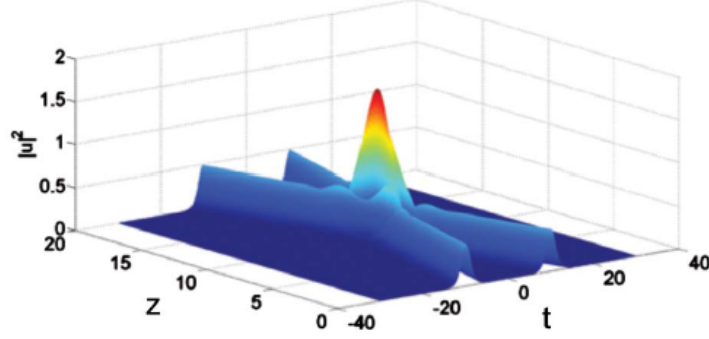


FIG. 21: The elastic collision between stable \mathcal{PT} -symmetric solitons with $\eta = 0.7$, boosted by frequency shift $\chi = \pm 5$ at $\gamma = 0.7$, see Eq. (103). The figure is shown as per Ref. [68].

shrinks to nil. The linearization of Eqs. (96) and (97) with $\gamma = 1$ around the NLSE solution (98) leads to the following equations for perturbations δu and δv :

$$\hat{L}(\delta u + i\delta v) = 0, \quad (104)$$

$$\hat{L}(\delta u - i\delta v) = -2i\kappa(\delta u + i\delta v), \quad (105)$$

where $\hat{L}\delta u \equiv [i\partial_z + (1/2)\partial_{tt} + 2|U|^2]\delta u + U^2\delta u^*$ is the NLSE linearization operator. If the underlying NLSE solution is stable by itself, Eq. (104) produces no instability, while Eq. (105) gives rise to a *resonance*, as $(\delta u + i\delta v)$ is a zero mode of operator \hat{L} . According to the linear-resonance theory [170], the respective perturbation $(\delta u - i\delta v)$ is unstable, growing $\sim z$ (rather than exponentially). Direct simulations of Eqs. (96) and (97) with $\gamma = 1$ confirm that the solitons are unstable, the character of the instability being consistent with its subexponential character [68].

The “supersymmetric” solitons may be stabilized by means of the *management* technique [171], which, in the present case, periodically reverses the common sign of the gain-loss and inter-core coupling coefficients, between $\gamma = K = +1$ and -1 (recall K is the coefficient of the inter-core coupling, which was scaled to be 1 above, and may now jump between $+1$ and -1). Flipping γ between $+1$ and -1 implies switch of the gain between the two cores, which is possible in the experiment. The coupling coefficient, κ , cannot flip by itself, but the signal in one core may pass π -shifting plates, which is tantamount to the periodic sign reversal of K .

Ansatz (98) still yields an exact solutions of Eqs. (96) and (97) with coefficients $\gamma = K$ subjected to the periodic management. On the other hand, the replacement of K by the

periodically flipping coefficient destroys the resonance in Eq. (105). In simulations, this management mode indeed maintains robust supersymmetric solitons [172].

V. CONCLUSION

Dual-core optical fibers is a research area which gives rise to a great variety of topics for fundamental theoretical and experimental studies, as well as to a plenty of really existing and potentially possible applications to photonics, including both traditional optics and plasmonics. While currently employed devices based on dual-core waveguides operate in the linear regime (couplers, splitters, etc.), the use of the intrinsic nonlinearity offers many more options, chiefly related to the use of self-trapped robust modes in the form of solitons. In terms of fundamental studies, solitons in dual-core fibers are the subject of dominant interest.

Theoretical studies of solitons in these systems had begun about three decades ago [3, 7–9, 20, 33–39, 48, 99, 105, 154, 155]. The earlier works and more recent ones have produced a great advancement in this field, with the help of analytical and numerical methods alike. The present article is focused on reviewing the results obtained, chiefly, in three most essential directions: the spontaneous symmetry breaking of solitons in couplers with identical cores and the formation of asymmetric solitons; the creation of stable dissipative solitons in gain-carrying nonlinear fibers (actually, fiber lasers), stabilized by coupling the active (pumped) core to a parallel lossy one; and the stability of solitons in \mathcal{PT} -symmetric couplers, with equal strengths of gain and loss carried by the parallel cores.

While the analysis of these areas has been essentially completed, taking into account both early and recent theoretical results, there remain many directions for the extension of the studies. In particular, a natural generalization of dual-core fibers is provided by multi-core arrays, which allow the creation of self-trapped modes which are discrete and continuous along the directions across the fiber array and along the fibers, respectively. These modes include semi-discrete solitons, which may be expected and used in many settings [173]-[177]. Another generalization implies the transition from 1D to 2D couplers, represented by dual-core planar optical waveguides. The consideration of spatiotemporal propagation in such a system makes it possible to predict the existence of novel species of 2D stable “light bullets” (spatiotemporal solitons [178]), such as spatiotemporal vortices [53], solitons realizing the

optical emulation of spin-orbit coupling [179, 180], and 2D \mathcal{PT} -symmetric solitons [180, 181].

The most challenging problem is that, as yet, there are very few experimental results reported for solitons in dual-core and multi-core systems. One of experimental findings is the creation of semi-discrete “light bullets” [182], including ones with embedded vorticity [183] (actually, in a transient form), in three-dimensional arrays of fiber-like waveguides permanently written in bulk samples of silica. Further development of experimental studies in this vast area is a highly relevant objective.

Acknowledgment

I thank Professor Gang-Ding Peng for his invitation to join the production of this volume, and to write the present article.

-
- [1] W. P. Huang, Coupled-mode theory for optical waveguides: an overview, *J. Opt. Soc. Am. A* **11**, 963-983 (1994).
 - [2] M. J. F. Digonnet and H. J. Shaw, Analysis of a tunable single-mode optical fiber coupler, *IEEE J. Quant. Electr.* **18**, 746-754 (1982).
 - [3] S. Trillo, S. Wabnitz, E. M. Wright, and G. I. Stegeman, Soliton switching in fiber nonlinear directional couplers, *Opt. Lett.* **13**, 672-674 (1988).
 - [4] K. Saitoh, Y. Sato, and M. Koshiba, Coupling characteristics of dual-core photonic crystal fiber couplers, *Opt. Exp.* **11**, 3188-3195 (2003).
 - [5] W. N. MacPherson, J. D. C. Jones, B. J. Mangan, J. C. Knight, and P. St. J. Russell, Two-core photonic crystal fibre for Doppler difference velocimetry, *Opt. Commun.* **223**, 375-380 (2003).
 - [6] S. M. Jensen, the nonlinear coherent coupler, *IEEE Journal of Quantum Electr.* **18**, 1580-1583 (1982); A. A. Maier, Optical transistors and bistable devices utilizing nonlinear transmission of light in systems with unidirectional coupled waves *Sov. J. Quant. Electron.* **12**, 1490-1494 (1982).
 - [7] S. R. Friberg, Y. Silberberg, M. K. Oliver, M. J. Andrejco, M. A. Saifi, and P. W. Smith, Ultrafast all-optical switching in dual-core fiber nonlinear coupler, *Appl. Phys. Lett.* **51**,

- 1135-1137 (1987).
- [8] S. R. Friberg, A. M. Weiner, Y. Silberberg, B. G. Sfez, and P. S. Smith, Femtosecond switching in dual-core-fiber nonlinear coupler, *Opt. Lett.* **13**, 904-906 (1988).
 - [9] D. R. Heatley, E. M. Wright, and G. I. Stegeman, Soliton coupler, *Appl. Phys. Lett.* **53**, 172-174 (1988).
 - [10] W. Królikowski and Y. S. Kivshar, Soliton-based optical switching in waveguide arrays, *J. Opt. Soc. Am. B* **13**, 876-887 (1996).
 - [11] S. C. Tsang, K. S. Chiang, and K. W. Chow, Soliton interaction in a two-core optical fiber, *Opt. Commun.* **229**, 431-439 (2004).
 - [12] I. M. Uzunov, R. Muschall, M. Göllés, Yu. S. Kivshar, B. A. Malomed, and F. Lederer, Pulse switching in nonlinear fiber directional couplers, *Phys. Rev. E* **51**, 25272537 (1995).
 - [13] F. Lederer, G. I. Stegeman, D. N. Christodoulides, G. Assanto, M. Segev, and Y. Silberberg, Discrete solitons in optics, *Phys. Rep.* **463**, 1-126 (2008).
 - [14] B. A. Malomed, G. D. Peng, and P. L. Chu, A nonlinear optical amplifier based on a dual-core fiber, *Opt. Lett.* **21**, 330-332 (1996).
 - [15] P. L. Chu, B. A. Malomed, and G. D. Peng, Passage of a pulse through a nonlinear amplifier, *Opt. Commun.* **140**, 289-295 (1997).
 - [16] H. E. Nistazakis, D. J. Frantzeskakis, J. Atai, B. A. Malomed, N. Efremidis, and K. Hizanidis, Multi-channel pulse dynamics in a stabilized Ginzburg-Landau system, *Phys. Rev. E* **65**, 036605 (2002).
 - [17] Y. D. Wu, Coupled-soliton all-optical logic device with two parallel tapered waveguides, *Fiber Integr. Opt.* **23**, 405-414 (2004).
 - [18] H. Hatami-Hanza, P. L. Chu, B. A. Malomed, and G. D. Peng, Soliton compression and splitting in double-core nonlinear optical fibers. *Opt. Commun.* **134**, 59-65 (1997).
 - [19] D. Chevriaux, R. Khomeriki, and J. Leon, Bistable transmitting nonlinear directional couplers, *Mod. Phys. Lett. B* **20**, 515-532 (2006).
 - [20] S. Trillo and S. Wabnitz, Coupling instability and power-induced switching with 2-core dual-polarization fiber nonlinear coupler, *J. Opt. Soc. Am. B* **5**, 483-491(1988).
 - [21] A. Villeneuve, C. C. Yang, P. C. J. Wigley, G. I. Stegeman, J. S. Aitchison, and C. N. Ironside, Ultrafast all-optical switching in semiconductor nonlinear directional couplers at half the band-gap, *Appl. Phys. Lett.* **61**, 147-149 (1992).

- [22] M. Hochberg, T. Baehr-Jones, C. Walker, and A. Scherer, Integrated plasmon and dielectric waveguides, *Opt. Exp.* **12**, 5481-5486 (2004).
- [23] J. Petráček, Nonlinear directional coupling between plasmonic slot waveguides, *Appl. Phys. B* **112**, 593-598 (2013).
- [24] D. A. Smirnova, A. V. Gorbach, I. V. Iorsh, I. V. Shadrivov, and Y. S. Kivshar, Nonlinear switching with a graphene coupler, *Phys. Rev. B* **88**, 045443 (2013).
- [25] W. C. K. Mak, B. A. Malomed, and P. L. Chu, Solitary waves in coupled nonlinear waveguides with Bragg gratings, *J. Opt. Soc. Am. B* **15**, 1685-1692 (1998).
- [26] Y. J. Tsofe and B. A. Malomed, Quasisymmetric and asymmetric gap solitons in linearly coupled Bragg gratings with a phase shift, *Phys. Rev. E* **75**, 056603 (2007).
- [27] Y. Sun, T. P. White, and A. A. Sukhorukov, Coupled-mode theory analysis of optical forces between longitudinally shifted periodic waveguides, *J. Opt. Soc. Am. B* **30**, 736-742 (2013).
- [28] G. D. Peng, P. L. Chu, and A. Ankiewicz, Soliton propagation in saturable nonlinear fiber couplers –variational and numerical results, *Int. J. Nonlin. Opt. Phys.* **3**, 69-87 (1994).
- [29] W. C. K. Mak, B. A. Malomed, and P. L. Chu, Soliton Coupling in Waveguide with Quadratic Nonlinearity, *Phys. Rev. E* **55**, 6134-6140 (1997).
- [30] A. Shapira, N. Voloch-Bloch, B. A. Malomed, and A. Arie, Spatial quadratic solitons guided by narrow layers of a nonlinear material, *J. Opt. Soc. Am. B* **28**, 1481-1489 (2011).
- [31] L. Albuch, B. A. Malomed, Transitions between symmetric and asymmetric solitons in dual-core systems with cubic-quintic nonlinearity, *Math. Comput. Simul.* **74**, 312-322 (2007).
- [32] X. Shi, B. A. Malomed, F. Ye, and X. Chen, Symmetric and asymmetric solitons in a nonlocal nonlinear coupler, *Phys. Rev. A* **85**, 053839 (2012).
- [33] A. W. Snyder, D. J. Mitchell, L. Poladian, D. R. Rowland, and Y. Chen, Physics of nonlinear fiber couplers, *J. Opt. Soc. Am. B* **8**, 2102-2112 (1991).
- [34] E. M. Wright, G. I. Stegeman, S. Wabnitz, Solitary-wave decay and symmetry-breaking instabilities in two-mode fibers, *Phys. Rev. A* **40**, 4455 (1989).
- [35] C. Paré and M. Florjańczyk, Approximate model of soliton dynamics in all-optical fibers, *Phys. Rev. A* **41**, 6287-6295 (1990).
- [36] A. I. Maimistov, Propagation of a light pulse in nonlinear tunnel-coupled optical waveguides, *Kvantovaya Elektron. (Moscow)* **18**, 758-761 (1991) [*Sov. J. Quant. Electr.* **21**, 687-690 (1991)].

- [37] P. L. Chu, B. A. Malomed, and G. D. Peng, Soliton switching and propagation in nonlinear fiber couplers: analytical results, *J. Opt. Soc. Am. B* **10**, 1379-1385 (1993).
- [38] N. Akhmediev and A. Ankiewicz, Novel soliton states and bifurcation phenomena in nonlinear fiber couplers, *Phys. Rev. Lett.* **70**, 2395-2398 (1993).
- [39] J. M. Soto-Crespo and N. Akhmediev, Stability of the soliton states in a nonlinear fiber coupler, *Phys. Rev. E* **48**, 4710-4715 (1993).
- [40] S. Trillo, G. Stegeman, E. Wright, and S. Wabnitz, Parametric amplification and modulational instabilities in dispersive nonlinear directional couplers with relaxing nonlinearity, *J. Opt. Soc. Am. B* **6**, 889-900 (1989).
- [41] R. S. Tasgal and B. A. Malomed, Modulational instabilities in the dual-core nonlinear optical fiber, *Physica Scripta* **60**, 418-422 (1999).
- [42] K. S. Chiang, Intermodal dispersion in two-core optical fibers, *Opt. Lett.* **20**, 997-999 (1995).
- [43] B. A. Malomed, I. M. Skinner, P. L. Chu, and G. D. Peng, Symmetric and asymmetric solitons in twin-core nonlinear optical fibers. *Phys. Rev. E* **53**, 4084-4091 (1996).
- [44] B. A. Malomed, Optical domain walls, *Phys. Rev. E* **50**, 1565-1571 (1994).
- [45] J. H. Li, K. S. Chiang, and K. W. Chow, Modulation instabilities in two-core optical fibers, *J. Opt. Soc. Am. B* **28**, 1693-1701 (2011).
- [46] D. Anderson, Variational approach to nonlinear pulse propagation in optical fibers, *Phys. Rev. A* **27**, 3135-3145 (1983).
- [47] D. Anderson, M. Lisak, and T. Reichel, Asymptotic propagation properties of pulses in a soliton-based optical-fiber communication system, *J. Opt. Soc. Am. B* **5**, 207-210 (1988).
- [48] M. Romagnoli, S. Trillo and S. Wabnitz, Soliton switching in nonlinear couplers, *Opt. Quantum Electron.* **24**, S1237-S1267 (1992).
- [49] B. A. Malomed, Variational methods in fiber optics and related fields, in: *Progr. Optics* **43**, 71-193 (E. Wolf, editor: North Holland, Amsterdam, 2002).
- [50] G. Herring, P. G. Kevrekidis, B. A. Malomed, R. Carretero-González, and D. J. Frantzeskakis, Symmetry breaking in linearly coupled dynamical lattices, *Phys. Rev. E* **76**, 066606 (2007).
- [51] Lj. Hadžievski, G. Gligorić, A. Maluckov, and B. A. Malomed, Interface solitons in one-dimensional locally coupled lattice systems, *Phys. Rev. A* **82**, 033806 (2010).
- [52] X. Shi, F. Ye, B. Malomed, and X. Chen, Nonlinear surface lattice coupler, *Opt. Lett.* **38**, 1064-1066 (2013).

- [53] N. Dror and B. A. Malomed, Symmetric and asymmetric solitons and vortices in linearly coupled two-dimensional waveguides with the cubic-quintic nonlinearity, *Physica D* **240**, 526-541 (2011).
- [54] K. E. Strecker, G. B. Partridge, A. G. Truscott, and R. G. Hulet, Bright matter wave solitons in Bose–Einstein condensates, *New J. Phys.* **5**, 73.1 (2003).
- [55] A. Gubeskys and B. A. Malomed, Symmetric and asymmetric solitons in linearly coupled Bose-Einstein condensates trapped in optical lattices, *Phys. Rev. A* **75**, 063602 (2007).
- [56] L. Salasnich, B. A. Malomed, and F. Toigo, Competition between the symmetry breaking and onset of collapse in weakly coupled atomic condensates, *Phys. Rev. A* **81**, 045603 (2010).
- [57] M. Matuszewski, B. A. Malomed, and M. Trippenbach, Spontaneous symmetry breaking of solitons trapped in a double-channel potential, *Phys. Rev. A* **75**, 063621 (2007).
- [58] C. J. Pethick and H. Smith, *Bose-Einstein Condensation in Dilute Gases*, Second edition (Cambridge University Press: Cambridge, UK, 2008).
- [59] M. van Hecke, Coherent and incoherent structures in systems described by the 1D CGLE: experiments and identification, *Physica D* **174**, 134-151 (2003).
- [60] P. Grellu and N. Akhmediev, Dissipative solitons for mode-locked lasers, *Nature Phot.* **6**, 84-92 (2012).
- [61] A. Sigler and B. A. Malomed, Solitary pulses in linearly coupled cubic-quintic Ginzburg-Landau equations, *Physica D* **212**, 305-316 (2005).
- [62] B. A. Malomed and H. G. Winful, Stable solitons in two-component active systems, *Phys. Rev. E* **53**, 5365 (1996).
- [63] J. Atai and B. A. Malomed, Stability and interactions of solitons in two-component systems, *Phys. Rev. E* **54**, 4371-4374 (1996).
- [64] J. Atai and B. A. Malomed, Exact stable pulses in asymmetric linearly coupled Ginzburg–Landau equations, *Phys. Lett. A* **246**, 412-422 (1998).
- [65] P. L. Chu, G. D. Peng, B. A. Malomed, H. Hatami-Hanza, and I. Skinner, Time domain soliton filter based on a semidissipative dual-core coupler, *Opt. Lett.* **20**, 1092-1094 (1995).
- [66] P. L. Chu, B. Malomed, and G. D. Peng, Passage of a pulse through a nonlinear amplifier, *Opt. Commun.* **140**, 289-295 (1997).
- [67] B. A. Malomed, Solitary pulses in linearly coupled Ginzburg-Landau equations, *Chaos* **17**, 037117 (2007).

- [68] R. Driben and B. A. Malomed, Stability of solitons in parity–time-symmetric couplers, *Opt. Lett.* **36**, 4323-4325 (2011).
- [69] N. V. Alexeeva, I. V. Barashenkov, A. A. Sukhorukov, and Y. S. Kivshar, Optical solitons in \mathcal{PT} -symmetric nonlinear couplers with gain and loss, *Phys. Rev. A* **85**, 063837 (2012).
- [70] C. M. Bender and S. Boettcher, Real spectra in non-Hermitian Hamiltonians having \mathcal{PT} symmetry, *Phys. Rev. Lett.* **80**, 5243-5246 (1998).
- [71] A. Ruschhaupt, F. Delgado, and J. G. Muga, Physical realization of \mathcal{PT} -symmetric potential scattering in a planar slab waveguide, *J. Phys. A: Math. Gen.* **38**, L171 (2005).
- [72] R. El-Ganainy, K. G. Makris, D. N. Christodoulides, and Z. H. Musslimani, Theory of coupled optical \mathcal{PT} -symmetric structures, *Opt. Lett.* **32**, 2632-2634 (2007).
- [73] M. V. Berry, Optical lattices with \mathcal{PT} symmetry are not transparent, *J. Phys. A* **41**, 244007 (2008).
- [74] Z. H. Musslimani, K. G. Makris, R. El-Ganainy, and D. N. Christodoulides, Optical solitons in \mathcal{PT} periodic potentials, *Phys. Rev. Lett.* **100**, 030402 (2008).
- [75] K. G. Makris, R. El-Ganainy, D. N. Christodoulides, and Z. H. Musslimani, Beam dynamics in \mathcal{PT} symmetric optical lattices, *Phys. Rev. Lett.* **100**, 103904 (2008).
- [76] S. Klaiman, U. Günther, and N. Moiseyev, Visualization of branch points in \mathcal{PT} -symmetric waveguides, *Phys. Rev. Lett.* **101**, 080402 (2008).
- [77] S. Longhi, Bloch Oscillations in Complex Crystals with \mathcal{PT} Symmetry, *Phys. Rev. Lett.* **103**, 123601 (2009).
- [78] C. M. Bender, Making sense of non-Hermitian Hamiltonians, *Rep. Prog. Phys.* **70**, 947 (2007).
- [79] K. G. Makris, R. El-Ganainy, D. N. Christodoulides, and Z. H. Musslimani, \mathcal{PT} -Symmetric Periodic Optical Potentials, *Int. J. Theor. Phys.* **50**, 1019-1041 (2011).
- [80] S. V. Suchkov, A. A. Sukhorukov, J. Huang, S. V. Dmitriev, C. Lee, and Y. S. Kivshar, Nonlinear switching and solitons in \mathcal{PT} -symmetric photonic systems, *Laser Photonics Rev.* **10**, 177-213 (2016).
- [81] V. V. Konotop, J. Yang, and D. A. Zezyulin, Nonlinear waves in \mathcal{PT} -symmetric systems, *Rev. Mod. Phys.* **88**, 035002 (2016).
- [82] B. A. Malomed, Evolution of nonsoliton and “quasiclassical” wavetrains in nonlinear Schrödinger and Korteweg - de Vries equations with dissipative perturbations, *Physica D* **29**, 155-172 (1987).

- [83] M. B. Mineev, G. S. Mkrtchyan, and V. V. Schmidt, On some effects in a system of 2 interacting Josephson junctions, *J. Low Temp. Phys.* **45**, 497-505 (1981).
- [84] Y. S. Kivshar and B. A. Malomed, Dynamics of fluxons in a system of coupled Josephson junctions, *Phys. Rev. B* **37**, 9325-9330 (1988).
- [85] A. V. Ustinov, H. Kohlstedt, M. Cirillo, N. F. Pedersen, G. Hallmanns, and G. Heiden, Coupled fluxon modes in stacked Nb/AlO_x/Nb long Josephson junctions, *Phys. Rev. B* **48**, 10614-10617 (1993).
- [86] Y. Makhlin, G. Schön, and A. Shnirman, Quantum-state engineering with Josephson-junction devices, *Rev. Mod. Phys.* **73**, 357-400 (2001).
- [87] S. Savel'ev, V. A. Yampol'skii, A. L. Rakhmanov, and F. Nori, Terahertz Josephson plasma waves in layered superconductors: spectrum, generation, nonlinear and quantum phenomena, *Rep. Prog. Phys.* **73**, 026501 (2010).
- [88] J. A. Gear and R. Grimshaw, Weak and strong-interactions between internal solitary waves, *Stud. Appl. Math.* **70**, 235-258 (1984).
- [89] B. A. Malomed, Leapfrogging solitons in a system of coupled Korteweg - de Vries equations, *Wave Motion* **9**, 401 (1987).
- [90] S. Y. Lou, B. Tong, H. C. Hu, and X. Y. Tang, Coupled KdV equations derived from two-layer fluids, *J. Phys. A: Math. Gen.* **39**, 513-527 (2006).
- [91] G. A. El, R. H. G. Grimshaw, and N. F. Smyth, Unsteady undular bores in fully nonlinear shallow-water theory, *Phys. Fluids* **18**, 027104 (2006).
- [92] A. Espinosa-Ceron, B. A. Malomed, J. Fujioka, and R. F. Rodriguez, Symmetry breaking in linearly coupled KdV systems, *Chaos* **22**, 033145 (2012).
- [93] G. Iooss and D. D. Joseph, *Elementary Stability and Bifurcation Theory* (Springer: Berlin, 1980).
- [94] J. P. Sabini, N. Finalyson, and G. I. Stegeman, All-optical switching in nonlinear X junctions, *Appl. Phys. Lett.* **55**, 1176-1178 (1989).
- [95] P. L. Chu, Yu. S. Kivshar, B. A. Malomed, G. D. Peng, and M. L. Quiroga-Teixeiro, Soliton controlling, switching, and splitting in fused nonlinear couplers, *J. Opt. Soc. Am. B* **12**, 898-903 (1995).
- [96] B. Mandal and A. R. Chowdhury, Solitary optical pulse propagation in fused fibre coupler – effect of Raman scattering and switching, *Chaos, Solitons and Fractals* **24**, 557-565 (2005).

- [97] V. V. Afanasjev, B. A. Malomed, and P. L. Chu, Dark soliton generation in a fused coupler, *Opt. Commun.* **137**, 229-232 (1997).
- [98] A. Boskovic, S. V. Chernikov, and J. R. Taylor, Spectral filtering effect of fused fiber couplers in femtosecond fiber soliton lasers, *J. Mod. Opt.* **42**, 1959-1963 (1995).
- [99] N. Akhmediev and A. Ankiewicz, Spatial soliton X-junctions and couplers, *Opt. Commun.* **100**, 186-192 (1993).
- [100] Y. Li, W. Pang, S. Fu, and B. A. Malomed, Two-component solitons under a spatially modulated linear coupling: Inverted photonic crystals and fused couplers, *Phys. Rev. A* **85**, 053821 (2012).
- [101] A. Harel and B. A. Malomed, Interactions of spatial solitons with fused couplers, *Phys. Rev. A* **89**, 043809 (2014).
- [102] G. P. Agrawal, *Nonlinear Fiber Optics*, Fourth edition (Academic Press: San Diego, 2007).
- [103] V. Rastogi, K. S. Chiang, and N. N. Akhmediev, Soliton states in a nonlinear directional coupler with intermodal dispersion, *Phys. Lett. A* **301**, 27-34 (2002).
- [104] L. D. Landau and E. M. Lifshitz, *Quantum Mechanics* (Nauka Publishers: Moscow, 1989).
- [105] A. Ankiewicz, N. Akhmediev, G. D. Peng, and P. L. Chu, *Opt. Commun.* **103**, 410 (1993).
- [106] F. Kh. Abdullaev, R. M. Abrarov, and S. A. Darmanyan, Dynamics of solitons in coupled optical fibers, *Opt. Lett.* **14**, 131-133 (1989).
- [107] Y. S. Kivshar and B.A. Malomed, Interaction of solitons in tunnel-coupled optical fibers, *Opt. Lett.* **14**, 1365-1367 (1989).
- [108] G. Cohen, Soliton interaction and stability in nonlinear directional fiber couplers, *Phys. Rev. E* **52**, 5565-5573 (1995).
- [109] I. M. Uzunov, R. Muschall, M. Gölles, Yu. S. Kivshar, B.A. Malomed, and F. Lederer, Pulse switching in nonlinear fiber directional couplers, *Phys. Rev. E* **51**, 2527-2537 (1995).
- [110] N. F. Smyth and A. L. Worthy, Dispersive radiation and nonlinear twin-core fibers, *J. Opt. Soc. Am. B* **14**, 2610-2617 (1997).
- [111] H. Sakaguchi and B. A. Malomed, Symmetry breaking of solitons in two-component Gross-Pitaevskii equations, *Phys. Rev. E* **83**, 036608 (2011).
- [112] S. L. Doty, J. W. Haus, Y. Oh, and R. L. Fork, Soliton interactions on dual-core fibers, *Phys. Rev. E* **51**, 709-717 (1995).
- [113] P. Li, L. Li, and B. A. Malomed, Multisoliton Newton's cradles and supersolitons in regular

- and parity-time-symmetric nonlinear couplers, *Phys. Rev. E* **89**, 062926 (2014).
- [114] G. D. Peng, B. A. Malomed, and P. L. Chu, 1998, Soliton collisions in a model of a dual-core nonlinear optical fiber. *Physica Scripta*, *Physica Scripta* **58**, 149-158 (1998).
- [115] D. J. Kaup, T. I. Lakoba, and B. A. Malomed, Asymmetric solitons in mismatched dual-core optical fibers, *J. Opt. Soc. Am. B* **14**, 1199-1206 (1997).
- [116] G. Arjunan, B. A. Malomed, M. Arumugam, and U. Ambikapathy, Modulational instability in linearly coupled asymmetric dual-core fibers, *Applied Sciences* **7**, 645 (2017).
- [117] D. J. Kaup and B. A. Malomed, Gap solitons in asymmetric dual-core nonlinear optical fibers. *J. Opt. Soc. Am. B* **15**, 2838-2846 (1998).
- [118] A. Zafrany, B. A. Malomed, and I. M. Merhasin, Solitons in a linearly coupled system with separated dispersion and nonlinearity, *Chaos* **15**, 037108 (2005).
- [119] J. Atai and B. A. Malomed, Bragg-grating solitons in a semilinear dual-core system, *Phys. Rev. E* **62**, 8713-8718 (2000).
- [120] A. R. Champneys, B. A. Malomed, J. Yang, and D. J. Kaup, "Embedded solitons": solitary waves in resonance with the linear spectrum, *Physica D* **152-153**, 340-354 (2001).
- [121] T. I. Lakoba, D. J. Kaup, and B. A. Malomed, Solitons in nonlinear fiber couplers with two orthogonal polarizations, *Phys. Rev. E* **55**, 6107 - 6120 (1997).
- [122] T. I. Lakoba and D. J. Kaup, Stability of solitons in nonlinear fiber couplers with two orthogonal polarizations, *Phys. Rev. E* **56**, 4791-4802 (1997).
- [123] C. M. de Sterke and J. E. Sipe, Gap solitons, *Progress in Optics* **33**, 203-260 (1994).
- [124] A. B. Aceves, Optical gap solitons: Past, present, and future; theory and experiments, *Chaos* **10**, 584-589 (2000).
- [125] Yu. I. Voloshchenko, Yu. N. Ryzhov, and V. E. Sotin, Stationary waves in nonlinear, periodically modulated media with large group retardation, *Zh. Tekh. Fiz.* **51**, 902-907 (1981) [*Sov. Phys. Tech. Phys.* **26**, 541-544 (1982)].
- [126] A. B. Aceves and S. Wabnitz, Self-induced transparency solitons in nonlinear refractive periodic media, *Phys. Lett. A* **141**, 37-42 (1989).
- [127] D. N. Christodoulides and R. I. Joseph, Slow Bragg solitons in nonlinear periodic structures, *Phys. Rev. Lett.* **62**, 1746-1749 (1989).
- [128] B. A. Malomed and R. S. Tasgal, Vibration modes of a gap soliton in a nonlinear optical medium, *Phys. Rev. E* **49**, 5787-5796 (1994).

- [129] I. V. Barashenkov, D. E. Pelinovsky, and E. V. Zemlyanaya, Phys. Rev. Lett. **80**, 5117 (1998).
- [130] A. De Rossi, C. Conti, and S. Trillo, Stability, Multistability, and Wobbling of Optical Gap Solitons, Phys. Rev. Lett. **81**, 85-88 (1998).
- [131] G. Burlak, S. Garcia-Paredes, and B. A. Malomed, \mathcal{PT} -symmetric couplers with competing cubic-quintic nonlinearities, Chaos **26**, 113103 (2016).
- [132] F. Smektala, C. Quemard, V. Couderc, and A. Barthélémy, Non-linear optical properties of chalcogenide glasses measured by Z-scan, J. Non-Cryst. Solids **274**, 232-237 (2000).
- [133] K. Ogusu, J. Yamasaki, S. Maeda, M. Kitao, and M. Minakata, Linear and nonlinear optical properties of Ag-As-Se chalcogenide glasses for all-optical switching, Opt. Lett. **29**, 265-267 (2004).
- [134] Kh. I. Pushkarov, D. I. Pushkarov, and I. V. Tomov, Self-action of light beams in nonlinear media: soliton solutions, Opt. Quant. Electr. **11**, 471-478 (1979).
- [135] S. Cowan, R. H. Enns, S. S. Rangnekar, and S. S. Sanghera, Quasi-soliton and other behaviour of the nonlinear cubic-quintic Schrödinger equation, Can. J. Phys. **64**, 311-315 (1986).
- [136] D. J. Richardson, J. Nilsson, and W. A. Clarkson, High power fiber lasers: current status and future perspectives, J. Opt. Soc. Am. B **27**, B63-B92 (2010).
- [137] P. Grelu and N. Akhmediev, Dissipative solitons for mode-locked lasers, Nature Phot. **6**, 84-92 (2012).
- [138] I. S. Aranson, L. Kramer, The world of the complex Ginzburg-Landau equation, Rev. Mod. Phys. **74**, 99-143 (2002).
- [139] B. A. Malomed, Complex Ginzburg-Landau equation, in: *Encyclopedia of Nonlinear Science*, pp. 157-160 (ed. by A. Scott; New York, Routledge, 2005).
- [140] L. M. Hocking and K. Stewartson, On the nonlinear response of a marginally unstable plane parallel flow to a two-dimensional disturbance, Proc. Roy. Soc. L. A **326**, 289-313 (1972).
- [141] N. R. Pereira, L. Stenflo, Nonlinear Schrödinger equation including growth and damping, Phys. Fluids **20**, 1733-1734 (1977).
- [142] V. I. Petviashvili, A. M. Sergeev, Spiral solitons in active media with excitation thresholds, Dokl. AN SSSR **276**, 1380-1384 (1984) [Sov. Phys. Doklady **29**, 493 (1984)].
- [143] W. van Saarloos and P. C. Hohenberg, Pulses and fronts in the complex Ginzburg-Landau equation near a subcritical bifurcation, Phys. Rev. Lett. **64**, 749-752 (1990).
- [144] B. A. Malomed and A. A. Nepomnyashchy, Kinks and solitons in the generalized Ginzburg-

- Landau equation, *Phys. Rev. A* **42**, 6009-6014 (1990).
- [145] V. Hakim, P. Jakobsen, and Y. Pomeau, Fronts vs. solitary waves in nonequilibrium systems, *Europhys. Lett.* **11**, 19-24 (1990).
- [146] P. Marcq, H. Chaté, and R. Conte, Exact solutions of the one-dimensional quintic complex Ginzburg-Landau equation, *Physica D* **73**, 305-317 (1994).
- [147] J. M. Soto-Crespo, N. N. Akhmediev, and V. V. Afanasjev, Stability of the pulselike solutions of the quintic complex Ginzburg-Landau equation, *J. Opt. Soc. Am. B* **13**, 1439-1449 (1996).
- [148] B. A. Malomed and H. G. Winful, Stable solitons in two-component active systems, *Phys. Rev. E* **53**, 5365-5368 (1996).
- [149] C. Li, G. Xu, L. Ma, N. Dou, and H. Gu, An erbium-doped fibre nonlinear coupler with coupling ratios controlled by pump power, *J. Opt. A: Pure Appl. Opt.* **7**, 540-543 (2005).
- [150] A. Marini, D. V. Skryabin, and B. A. Malomed, “Stable spatial plasmon solitons in a dielectric-metal-dielectric geometry with gain and loss”, *Opt. Exp.* **19**, 6616-6622 (2011).
- [151] W. J. Firth and P. V. Paulau, Soliton lasers stabilized by coupling to a resonant linear system, *Eur. Phys. J. D* **59**, 13-21 (2010).
- [152] P. V. Paulau, D. Gomila, P. Colet, N. A. Loiko, N. N. Rosanov, T. Ackemann, and W. J. Firth, Vortex solitons in lasers with feedback, *Opt. Exp.* **18**, 8859-8866 (2010).
- [153] P. V. Paulau, D. Gomila, P. Colet, B. A. Malomed, and W. J. Firth, From one- to two-dimensional solitons in the Ginzburg-Landau model of lasers with frequency-selective feedback, *Phys. Rev. E* **84**, 036213 (2011).
- [154] H. G. Winful and D. T. Walton, Passive mode locking through nonlinear coupling in a dual-core fiber laser, *Opt. Lett.* **17**, 1688-1690 (1992).
- [155] D. T. Walton and H. G. Winful, Passive mode locking with an active nonlinear directional coupler: positive group-velocity dispersion, *Opt. Lett.* **18**, 720-722 (1993).
- [156] E. Marti-Panameno, L. C. Gomez-Pavon, A. Luis-Ramos, M. M. Mendez-Otero, M. D. I. Castillo, Self-mode-locking action in a dual-core ring fiber laser, *Opt. Commun.* **194**, 409-414 (2001).
- [157] P. L. Chu, G. D. Peng, B. A. Malomed, H. Hatami-Hansa, and I. M. Skinner, Time domain soliton filter based on a semidissipative dual-core coupler, *Opt. Lett.* **20**, 1092-1094 (1995).
- [158] J. Atai and B. A. Malomed, Stability and interactions of solitons in two-component systems, *Phys. Rev. E* **54**, 4371-4374 (1996).

- [159] J. Atai, B. A. Malomed, Exact stable pulses in asymmetric linearly coupled Ginzburg-Landau equations, *Phys. Lett. A* **246**,412-422 (1998).
- [160] Yu. S. Kivshar and B. A. Malomed, Dynamics of solitons in nearly integrable systems, *Rev. Mod. Phys.* **61**, 763-915 (1989).
- [161] N. Efremidis, K. Hizanidis, B. A. Malomed, H. E. Nistazakis, and D. J. Frantzeskakis, Stable transmission of solitons in the region of normal dispersion, *J. Opt. Soc. Am. B* **17**, 952-958 (2000).
- [162] J. Atai and B. A. Malomed, Bound states of solitary pulses in linearly coupled Ginzburg-Landau equations, *Phys. Lett. A* **244**, 551-556 (1998).
- [163] N. Efremidis, K. Hizanidis, H. E. Nistazakis, D. J. Frantzeskakis, and B. A. Malomed, Stabilization of dark solitons in the cubic Ginzburg-Landau equation, *Phys. Rev. E* **62**, 7410-7414 (2000).
- [164] R. Ganapathy, B. A. Malomed, and K. Porsezian, Modulational instability and generation of pulse trains in asymmetric dual-core nonlinear optical fibers, *Phys. Lett. A* **354**, 366-372 (2006).
- [165] K. Nozaki and N. Bekki, Exact Solutions of the Generalized Ginzburg-Landau Equation, *J. Phys. Soc. Jpn.* **53**, 1581-1582 (1984).
- [166] H. Sakaguchi, Hole solutions in the complex Ginzburg-Landau equation near a subcritical bifurcation, *Progr. Theor. Phys.* **86**, 7-12 (1991).
- [167] H. Sakaguchi and B. A. Malomed, Breathing and randomly walking pulses in a semilinear Ginzburg-Landau system, *Physica D* **147**, 273-282 (2000).
- [168] A. Guo, G. J. Salamo, D. Duchesne, R. Morandotti, M. Volatier-Ravat, V. Aimez, G. A. Siviloglou, and D. N. Christodoulides, Observation of \mathcal{PT} -symmetry breaking in complex optical potentials, *Phys. Rev. Lett.* **103**, 093902 (2009).
- [169] C. E. Ruter, K. G. Makris, R. El-Ganainy, D. N. Christodoulides, M. Segev, and D. Kip, "Observation of parity-time symmetry in optics", *Nature Physics* **6**, 192-195 (2010).
- [170] L. D. Landau and E. M. Lifshitz, *Mechanics* (Nauka Publishers: Moscow, 1988).
- [171] B. A. Malomed, *Soliton Management in Periodic Systems* (Springer: New York, 2006).
- [172] R. Driben and B. A. Malomed, Stabilization of solitons in \mathcal{PT} models with supersymmetry by periodic management, *EPL* **96**, 51001 (2011).
- [173] A. B. Aceves, C. De Angelis, A. M. Rubenchik, and S. K. Turitsyn, Multidimensional solitons

- in fiber arrays, *Opt. Lett.* **19**, 329-331 (1994).
- [174] A. B. Aceves, C. De Angelis, G. G. Luther, and A. M. Rubenchik, *Opt. Lett.* **19**, 1186-1188 (1994).
- [175] A. B. Aceves, G. G. Luther, C. De Angelis, A. M. Rubenchik, and S. K. Turitsyn, Energy localization in nonlinear fiber arrays: collapse-effect compressor, *Phys. Rev. Lett.* **75**, 73-76 (1995).
- [176] M. Matsumoto, S. Katayama, and A. Hasegawa, Optical switching in nonlinear waveguide arrays with a longitudinally decreasing coupling coefficient, *Opt. Lett.* **20**, 1758-1760 (1995).
- [177] R. Blit and B. A. Malomed, Propagation and collisions of semidiscrete solitons in arrayed and stacked waveguides, *Phys. Rev. A* **86**, 043841 (2012).
- [178] Y. Silberberg, Collapse of optical pulses, *Opt. Lett.* **22**, 1282-1284 (1990).
- [179] Y. V. Kartashov, B. A. Malomed, V. V. Konotop, V. E. Lobanov, and L. Torner, Stabilization of solitons in bulk Kerr media by dispersive coupling, *Opt. Lett.* **40**, 1045-1048 (2015).
- [180] H. Sakaguchi and B. A. Malomed, One- and two-dimensional solitons in \mathcal{PT} -symmetric systems emulating spin-orbit coupling, *New J. Phys.* **18**, 105005 (2016).
- [181] G. Burlak and B. A. Malomed, Stability boundary and collisions of two-dimensional solitons in \mathcal{PT} -symmetric couplers with the cubic-quintic nonlinearity, *Phys. Rev. E* **88**, 062904 (2013).
- [182] S. Minardi, F. Eilenberger, Y. V. Kartashov, A. Szameit, U. Röpke, J. Kobelke, K. Schuster, H. Bartelt, S. Nolte, L. Torner, F. Lederer, A. Tünnermann, and T. Pertsch, Three-dimensional light bullets in arrays of waveguides, *Phys. Rev. Lett.* **105**, 263901 (2010).
- [183] F. Eilenberger, K. Prater, S. Minardi, R. Geiss, U. Röpke, J. Kobelke, K. Schuster, H. Bartelt, S. Nolte, A. Tünnermann, and T. Pertsch, Observation of discrete, vortex light bullets, *Phys. Rev. X* **3**, 041031 (2013).